Ευρωπαϊκή Ένωση
Ευρωπαϊκό Κοινωνικό Ταμείο
ΕΠΙΧΕΙΡΗΣΙΑΚΟ ΠΡΟΓΡΑΜΜΑ
ΕΚΠΑΙΔΕΥΣΗ ΚΑΙ ΔΙΑ ΒΙΟΥ ΜΑΘΗΣΗ
επένδυση στην κοινωνία της γνώσης
ΥΠΟΥΡΓΕΙΟ ΠΑΙΔΕΙΑΣ & ΘΡΗΣΚΕΥΜΑΤΩΝ, ΠΟΛΙΤΙΣΜΟΥ & ΑΘΛΗΤΙΣΜΟΥ
ΕΙΔΙΚΗ ΥΠΗΡΕΣΙΑ ΔΙΑΧΕΙΡΙΣΗΣ
Με τη συγχρηματοδότηση της Ελλάδας και της Ευρωπαϊκής Ένωσης
ΕΣΠΑ 2007-2013
πρόγραμμα για την ανάπτυξη
ΕΥΡΩΠΑΪΚΟ ΚΟΙΝΩΝΙΚΟ ΤΑΜΕΙΟ

Technical University of Crete
Electronics & Computer Engineering Dept.
Electronics Laboratory
Optoelectronics Group

# IN VIVO MOLECULAR IMAGING OF EPITHELIAL PRE-CANCERS BASED ON DYNAMIC OPTICAL SCATTERING MODELING

**George Papoutsoglou**

# INTRODUCTION

Motivation
Emerging technologies
Dynamic Contrast-Enhanced Optical Imaging (DCE-OI)
Clinical evidence
Scope
Outline of the project

# Motivation

## Problems in current diagnostic chain for the early detection of cancer lesions

- Qualitative
- Subjective
- High inter-observer disagreement
- limited diagnostic performance at each step
- additional steps increase complexity and costs

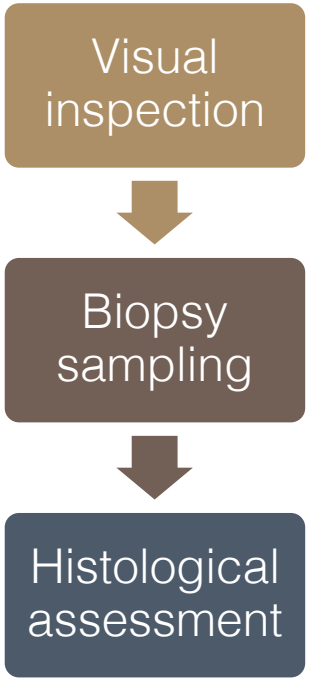

Crow, *Nature*, 2012

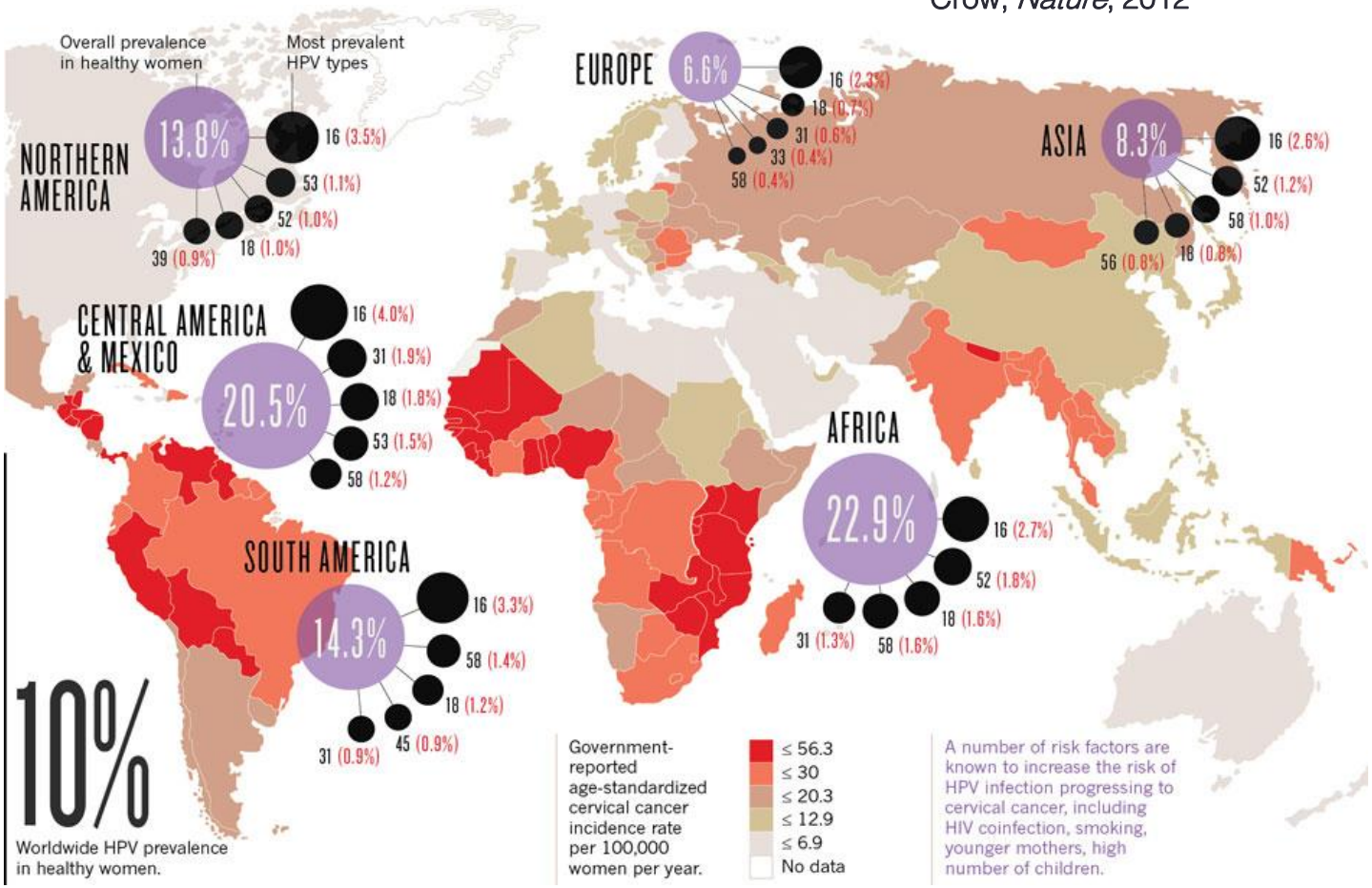


- Developed world
  - poor cost-effectiveness
- Low resource countries
  - inability to implement and sustain such complicated prevention programs

# Dynamic Contrast-Enhanced Optical Imaging (DCE-OI)

## Introduced for the first time by C. Balas in the late 90's

C. J. Balas, et al., "*In vivo detection and staging of epithelial dysplasias and malignancies based on the quantitative assessment of acetic acid-tissue interaction kinetics*," J. Photochem. Photobiol. B-Biology, vol. 53, no. 1–3, pp. 153–157, 1999.

C. Balas, "*A novel optical imaging method for the early detection, quantitative grading, and mapping of cancerous and precancerous lesions of cervix*," IEEE Trans Biomed Eng, vol. 48, no. 1, pp. 96–104, 2001.

- **Dynamic effects**
  - Information-rich
  - Signal profile: identify false positives
    - Inflammatory tissues
    - Repairing epithelium
    - Metaplasia

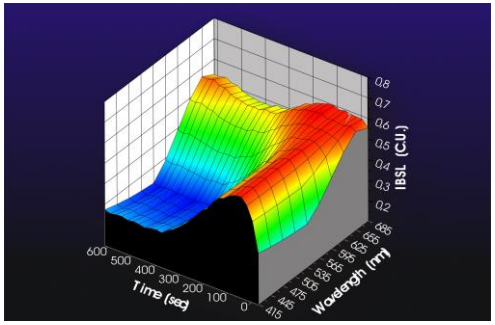


- **Spectral Imaging**
  - Discriminate between responsive and non responsive areas
  - Assess alterations in light scattering properties of the tissue

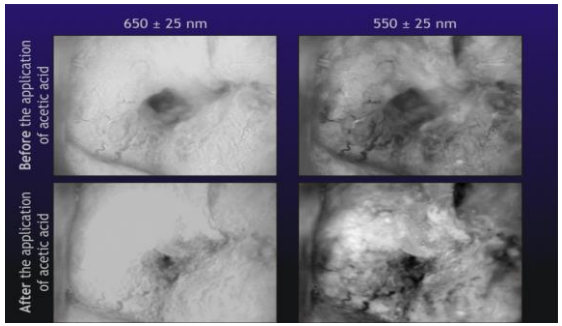

# DCE-OI principle

spatio-temporal recording of biomarker-tissue interaction ***in-vivo***, **non-invasively** and **in real time**.

clinical setup

Snapshot Spectral Imaging

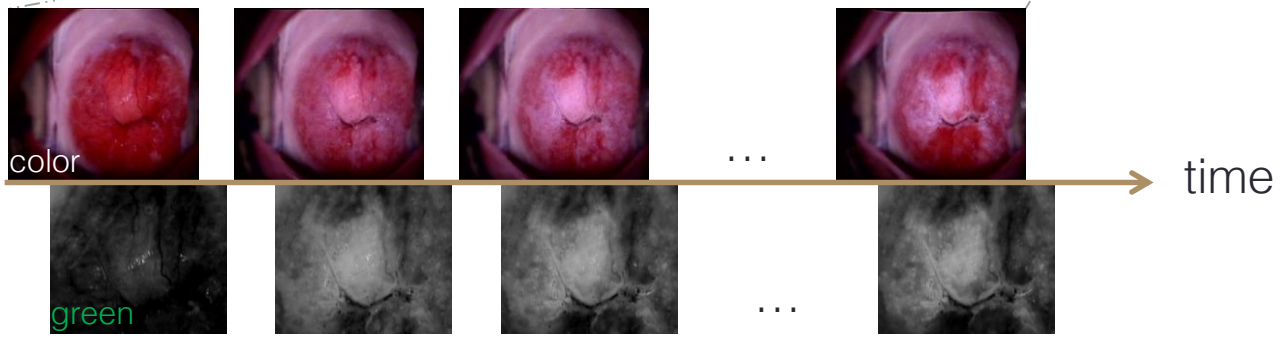


pixel-by-pixel recordings

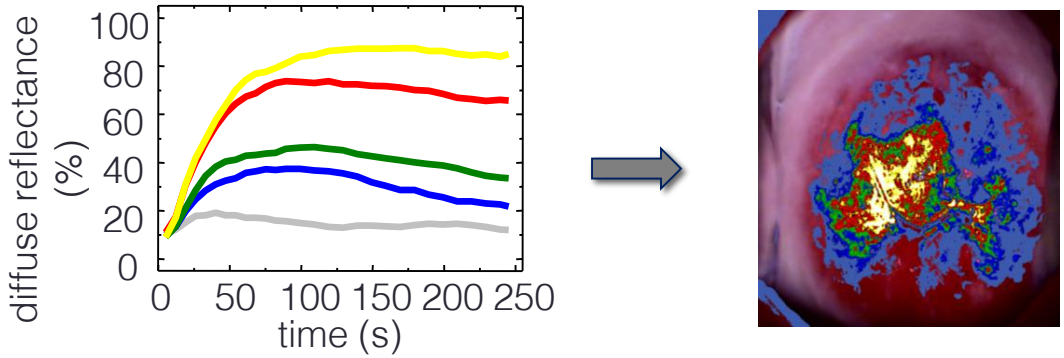

# Clinical evidence


http://www.dysismedical.com/the-science.aspx

**Trial profile** (Phase II)

**Hospitals**: Hammersmith (London, UK) St. Mary's (London, UK) Alexandra (Athens, GR)

**Aim**: To compare the performance of DySIS with the performances of conventional colposcopy and cytology in detecting High Grade CIN

**Recruitment**: 447 women with abnormal smear

| | DySIS | Conventional Colposcopy | Referral Cytology |
|---|---|---|---|
| Sensitivity | 79% | 49% | 53% |
| Specificity | 76% | 89% | 86% |
| Diagnostic Odds Ratio | 11.81 | 7.91 | 6.88 |

Soutter W.P., et al., *Clinical Cancer Research*, 2009

# Technology awareness

- **Standard care worldwide**
  - Europe
    CE-Marked
    Greece, UK, Netherlands, Sweden, France, …
  - USA
    FDA approval, 2011
- **Prizes**
  - Medilink Innovation Award, 2013
  - Scottish Life Science Award, 2013


## Integrates the most promising sciences

- Molecular Imaging
  - Imaging of specific tissue-marker interactions
- Spectral Imaging
  - Using specific color bands for enhanced imaging
- Dynamic Imaging
  - Recording the changes of tissue characteristics over time

……. without changing screening standard procedures

# Going one step further

**Exact origins of the phenomenon had been largely unknown**

## DCE-OI

- Dynamic optical signals are correlated with neoplasia progression
- Dynamic effects are information-rich
  - Transport pathways
  - Reversible pharmacodynamics
- Renders possible the systematic, model-based quantitative assessment of several biological parameters that are determining the features of the experimental data

## Scope

- Interpret and correlate the optical phenomenon with the underlying functional and structural alterations
- Mine diagnostic information by solving the inverse problem

# Project pipeline

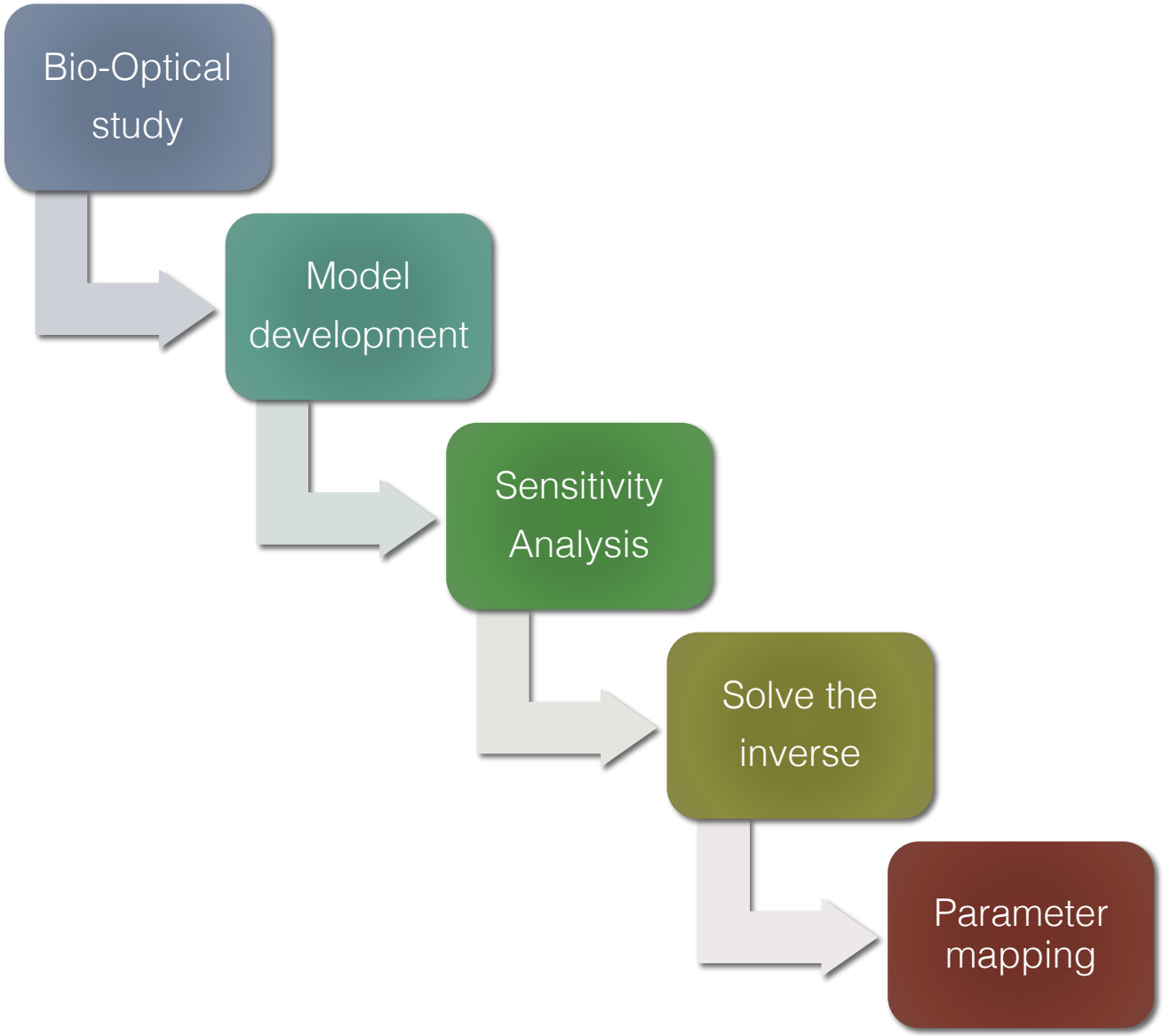

# BACKGROUND, STATE OF THE ART

- Strategy for modeling metabolic systems
- Epithelial pharmacodynamics/pharmacokinetics
- Identifiability
- Solution of the inverse problem

# Epithelia neoplasia of the cervix

- During a woman's lifespan the columnar epithelium of the endocervix is converted progressively to squamous
- CIN tends to form in the vicinity of the Transformation Zone (TZ).

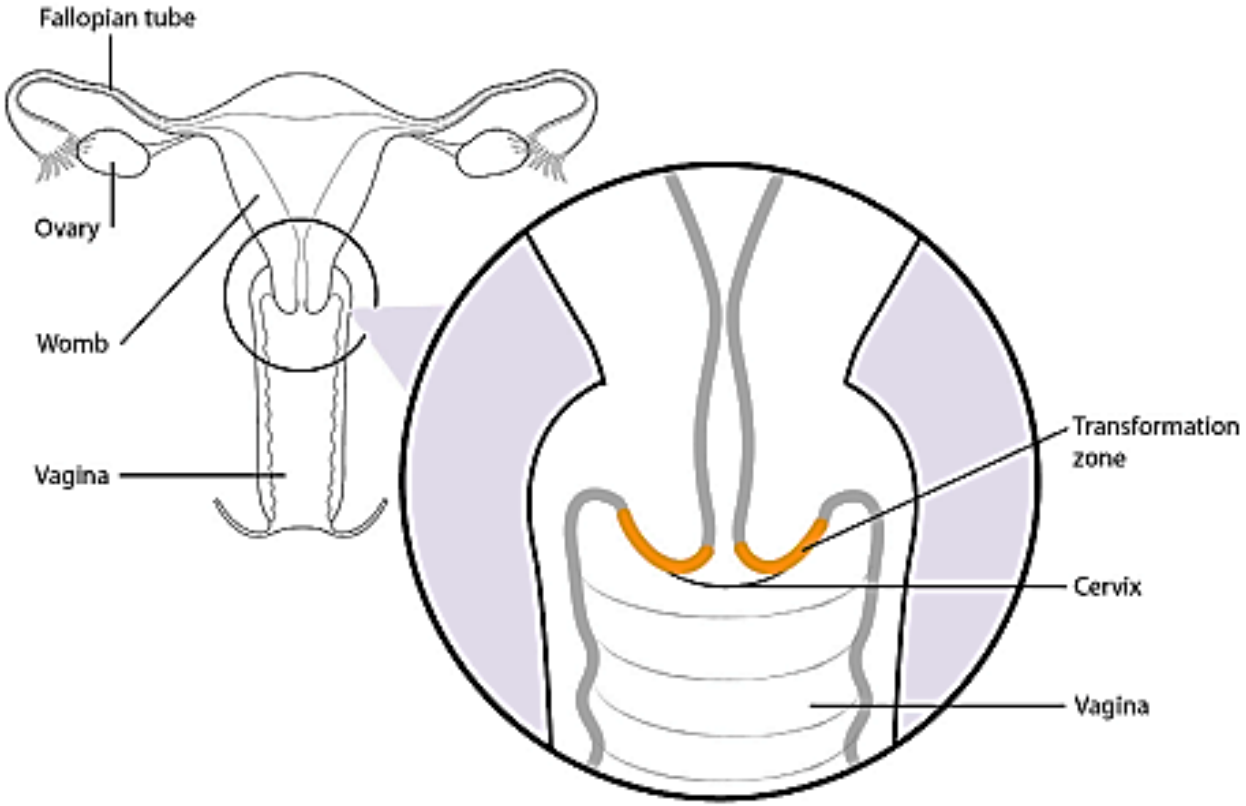

# Structural and functional changes during CIN

- **Structural changes**
  - tissue homogenization
  - smaller cell size
  - larger nuclei
  - larger extracellular space

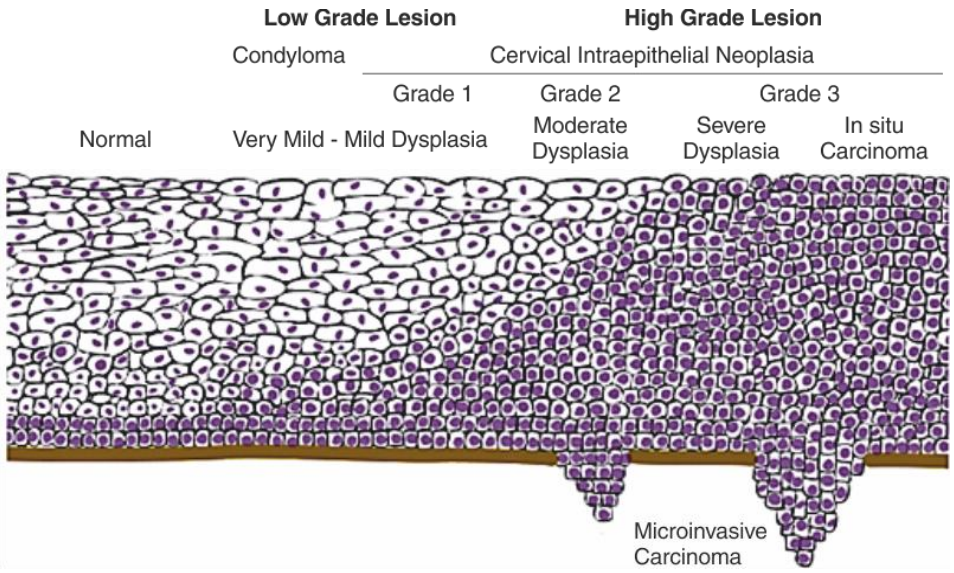


- **Functional changes**
  - increased production and proliferation rate
  - Tight Junctions
    - greater diffusivity
  - Gap Junctions
    - reduced cell-to-cell cross talking
    - quit metabolic cooperation
  - pH regulation
    - low extracellular pH
    - normal intracellular pH

# The tissue in terms of structure and function

## Classification

- Columnar
- Squamous
- Transitional
- **Stratified squamous**

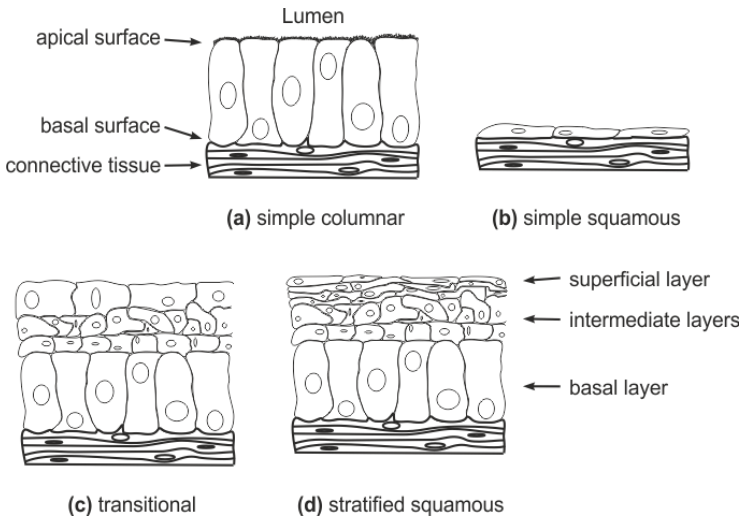


## Adhesion and communication

- Plasma membrane
  - Secretion-Absorption: **transcellular**
  - Diffusion: Passive, Active
- Tight junctions
  - Protection: **paracellular**
  - Diffusion: Passive, Size and charge selective
- Gap junctions
  - Communication - Metabolic cooperation: **intercellular**
  - Diffusion: Passive, Size and charge selective

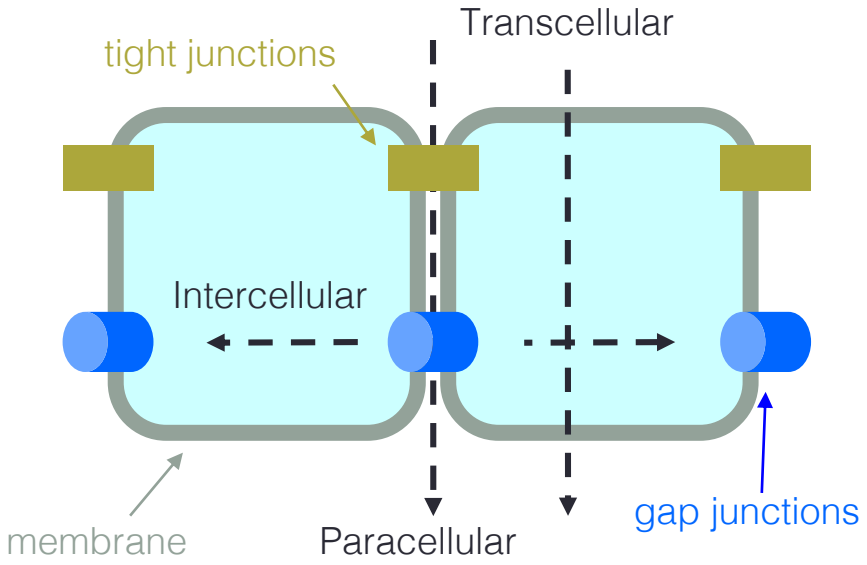

# Maintaining the pH

- **Short-term mechanisms**
  - physicochemical buffering
  - metabolism:
    - organelles
    - metabolic cooperation
- **Long-term mechanisms**
  - Ion pumps

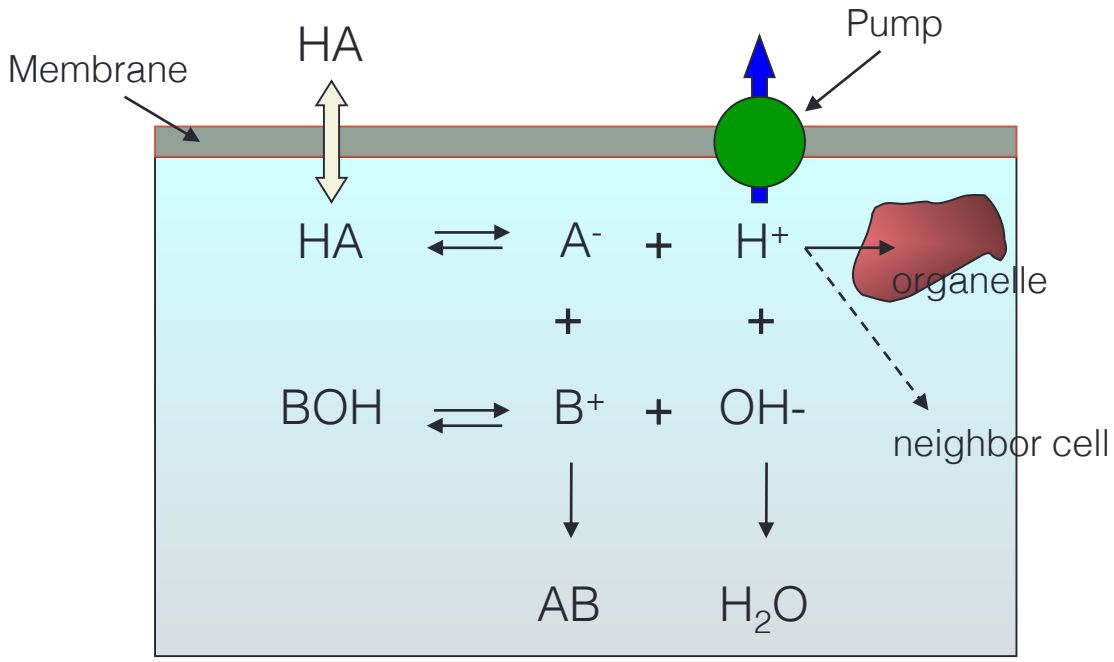

# Mathematical representation

## Compartmental models

- clustering of the spatially distributed similar information in a tractable discrete topology
- deterministic
- linear or non-linear

## interconnection = material flux

- transport from one location to another (diffusion)
- chemical reaction/transformation

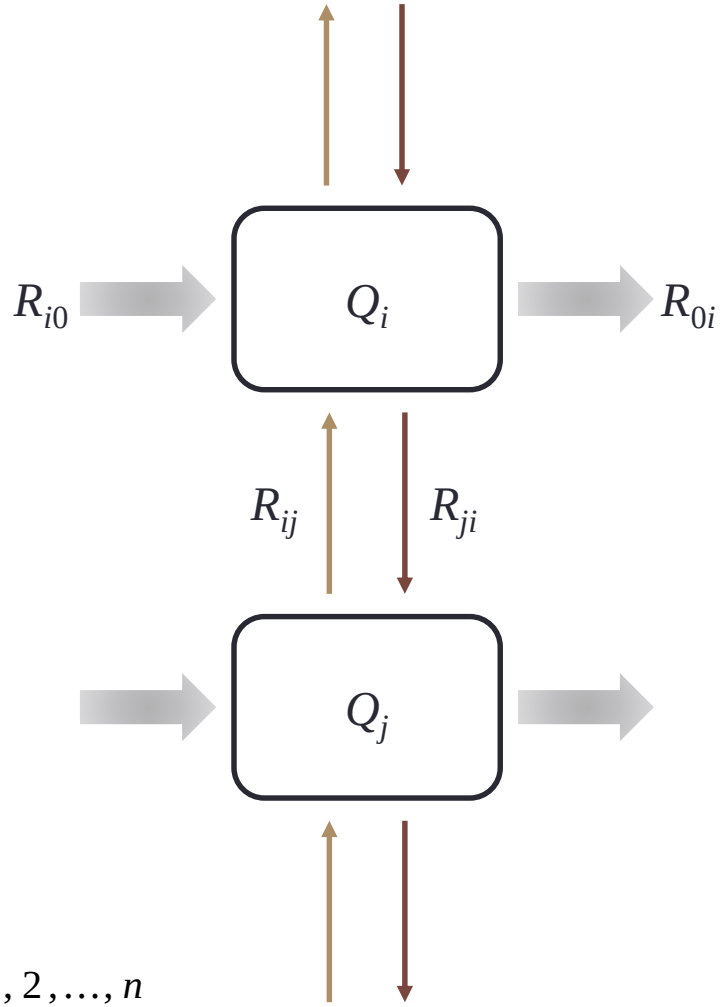


## Conservation law

$$\frac{dQ_i}{dt} = R_{i0} + \sum_{\substack{j=1 \\ j\neq i}}^{n} R_{ij} - \sum_{\substack{j=1 \\ j\neq i}}^{n} R_{ji} - R_{0i}, \quad i = 1, 2, \ldots, n$$

# Biophysical Laws

flux = mobility x concentration x driving force → $J^{(S)} = U^{(S)} C^{(S)} \left( -\frac{d\mu^{(S)}}{dx} \right)$

## Fick's first law

$$J^{(S)}_{\mathrm{I}\to\mathrm{II}} = P^{(S)} \left( [S]^{\mathrm{I}} - [S]^{\mathrm{II}} \right)$$

## Goldman–Hodgkin–Katz (GHK) equation

$$J^{(S)}_{\mathrm{I}\to\mathrm{II}} = \frac{z_S F V_m}{RT \left( 1 - e^{-z_S F V_m / RT} \right)} P^{(S)} \left( [S]^{\mathrm{I}} - [S]^{\mathrm{II}} e^{-z_S F V_m / RT} \right)$$

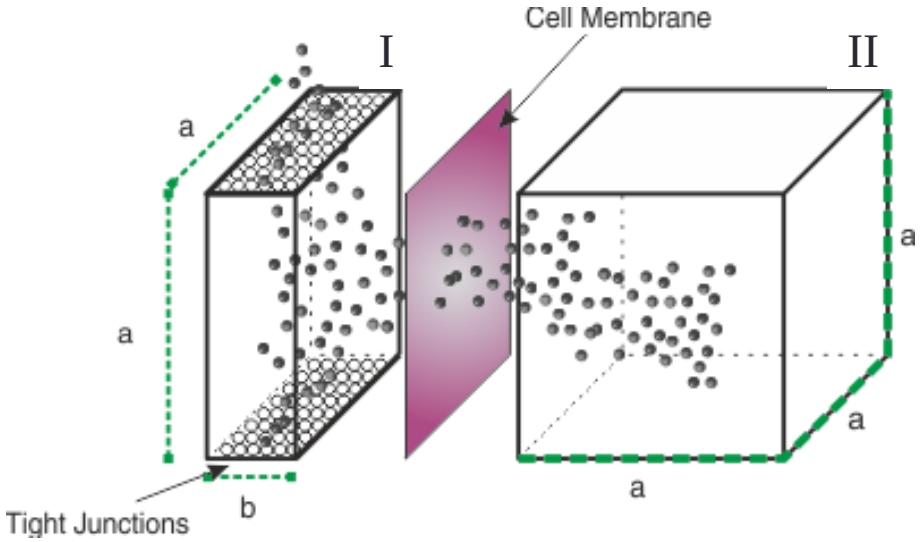


- Constant flux over a given surface area ($A$)
- Constant concentration over a volume ($V$)

$$\frac{dc}{dt} = -\frac{A}{V} J$$

# Towards the solution of the inverse problem

- ✓ Strong biological background
- ✓ Suitable model

} address the inverse problem (parameter estimation), directly

## Caveat

- uncertain model structure and/or parameters
- mathematically interacting and/or correlated parameters

## Question:

*Can the unknown system parameters be uniquely estimated from the available experimental data and using the proposed model's structure*?

## Theoretical study

- sensitivity
- identifiability
- estimability

} 

- reduce the parameter complexity
- improve the posedness of the inverse problem.

# Parameter identifiability

- **Parameter types**
  - Structural: inherent to the structural equations
  - Experimental: imposed by experimental conditions
  - Observational: captured by the observations
- **Global identifiability**
  - Observational ≡ Structural (unique)
  - linear models
    - algebraic manipulations
    - transformations (Laplace, similarity transformations)
  - non-linear models
    - Differential algebra
    - Expansions (Taylor series, Lie derivatives)
- **Local identifiability**
  - Observational ⊂ Structural (not unique)
  - Local sensitivity analysis
  - Global Sensitivity Analysis
    - Model reduction/restructuring
    - Parameter ranking

# Sensitivity analysis in dynamic system models

## Local sensitivity analysis

1. derivative at a "base point"
2. local sensitivity matrix (Jacobian)

$$\mathbf{S}_D = \begin{bmatrix} \left.\frac{\partial \hat{\mathbf{y}}}{\partial p_1}\right|_{t_1} & \cdots & \left.\frac{\partial \hat{\mathbf{y}}}{\partial p_j}\right|_{t_1} \\ \vdots & \ddots & \vdots \\ \left.\frac{\partial \hat{\mathbf{y}}}{\partial p_1}\right|_{t_s} & \cdots & \left.\frac{\partial \hat{\mathbf{y}}}{\partial p_j}\right|_{ts} \end{bmatrix}$$

3. parameter assessments
   - Linear (e.g. Pearson's)
   - Principal Component Analysis (PCA)
   - Fisher Information Matrix (FIM)

## Global sensitivity analysis

- parameters ⟶ random variables
- No analytic in/output relationship and/or model additivity is required
- **Variance-based methods**
  - decompose the output variance into terms of increasing dimensionality:

$$V(\mathrm{Y}) = \sum_{i=1}^{N} V_i + \sum_{i}\sum_{j} V_{ij} + \sum_{i}\sum_{j}\sum_{k} V_{ijk} + \ldots + V_{1,2,\ldots,\mathrm{k}}$$

  - robust statistical inferences
  - condensed format

First Order Sensitivity (FOS):

$$S_i = V_i / V(\mathbf{Y})$$

Total Order Sensitivity (TOS):

$$S_{Ti} = S_i + S_{ij} + \ldots + S_{ij..k}$$

# Method of Sobol'

- **Conditional variances as multidimensional integrals**
- **Quasi - Monte Carlo procedure:**
  1. Generate a $N_{sample}$ x $2k$ matrix using low discrepancy number sequences e.g. $LP_T$
  2. Split into a sample ($\mathbf{A}^k$) and a re-sample ($\mathbf{B}^k$) matrix
  3. Form the $\mathbf{A_B}^{(i)}$ and $\mathbf{B_A}^{(i)}$ matrices
     - First order sensitivity (FOS)

$$V_{X_i}\left(E_{\mathbf{X}\sim i}\left(Y\left|X_i\right.\right)\right) = \frac{1}{N_{sample}}\sum_{j=1}^{N_{sample}} f(\mathbf{B})_j\left(f\left(\mathbf{A}_{\mathbf{B}}^{(i)}\right)_j - f(\mathbf{A})_j\right)$$

     - Total order sensitivity (TOS)

$$E_{\mathbf{X}\sim i}\left(V_{X_i}\left(Y\left|\mathbf{X}_{\sim i}\right.\right)\right) = \frac{1}{2N_{sample}}\sum_{j=1}^{N_{sample}}\left(f(\mathbf{A})_j - f\left(\mathbf{A}_{\mathbf{B}}^{(i)}\right)_j\right)^2$$

Both FOS and TOS indexes have been calculated for every time instance lapsed after the initiation of the phenomenon

# Theoretical identifiability analysis

**FOS**: parameter ranking

high ranking 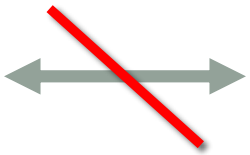 identifiability

**TOS**: designate non-essential parameters

- nullity (or inferiority to an empirical threshold)
- non-injectivity

Non-identifiability may be assesed from:

- linear dependence of the TOS with respect to time
  - correlation = ±1
  - repeatedly remove one unidentifiable parameter each time, until no more unidentifiable parameters remain
- parameter interactions

# Parameter estimation

**Let the most identifiable parameter set (p) be defined**

**Optimization of a cost function (likelihood), $J(\mathbf{p}) = L(\mathbf{p}|\mathbf{z})$**

## Frequentist approach

Find the set **p** that gives the highest probability to the observed data

- assumption on error
- maximum likelihood methods

Special case:

independent, additive Gaussian noise with zero mean and constant variance

$$J(\mathbf{p}) = \sum_{i=1}^{n_y} \sum_{t=t_0}^{t_{max}} \left( \frac{z_i^*(t) - z_i(t,\mathbf{p})}{\sigma_i} \right)^2$$

Minimization methodologies

- linear/non-linear least squares
- heuristic search

# Global optimization

- **Deterministic strategies**
- **Stochastic strategies**

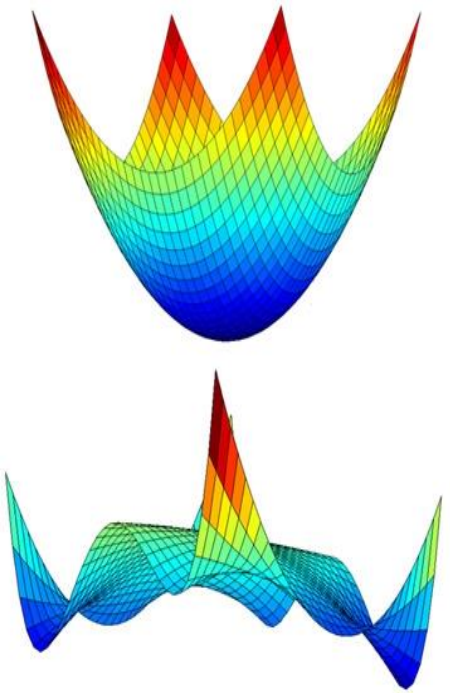

**Model: multi-resolution design**

- Non-Convex
- no analytical representation
- non factorable equations

direct-search (derivative-free) GO methods are mostly suitable

# Roadmap

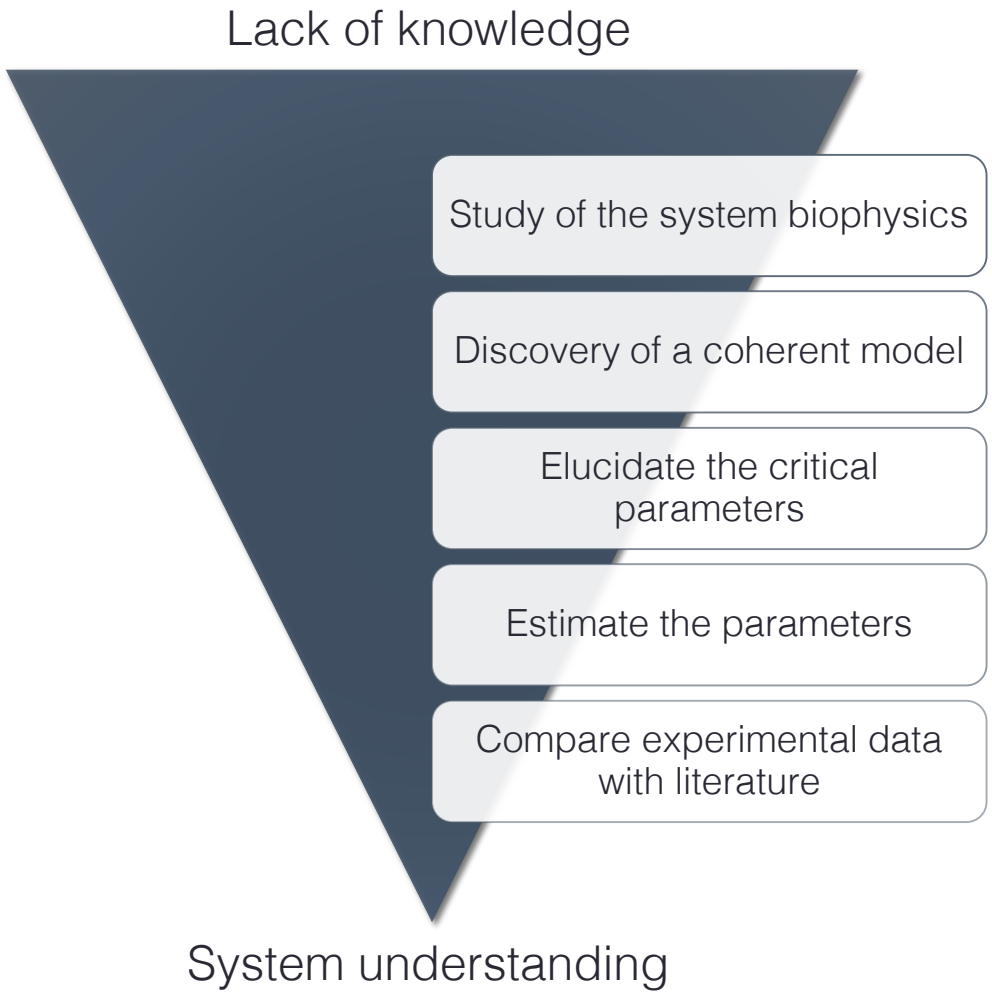
Lack of knowledge
Study of the system biophysics
Discovery of a coherent model
Elucidate the critical parameters
Estimate the parameters
Compare experimental data with literature
System understanding

Bio-Optical study

Mathematical Implementation

Sensitivity Analysis

Solve the inverse

Parameter mapping

# THESIS RESULTS & CONTRIBUTIONS

## 1. BIO-OPTICAL MODEL DESIGN

Biomarker pharmacodynamics

The “ouzo effect”

Interpretation of the optical excitation

# Result 1: The origin of the bio-optical phenomenon

- We present the link between metabolic processes, biomarker pharmacodynamics/kinetics and the provoked dynamic, macroscopic phenomenon

- The phenomenon's dynamics is not determined by the intrinsic time characteristics of the conformational changes, but from the dynamic characteristics of the change causing factor instead.

**Relevant publications**

C. Balas, G. Papoutsoglou, and A. Potirakis, "*In vivo molecular imaging of cervical neoplasia using acetic acid as biomarker*," IEEE J. Sel. Top. Quantum Electron., vol. 14, no. 1, pp. 29–42, 2008

# Biophysical interpretation of phenomenon

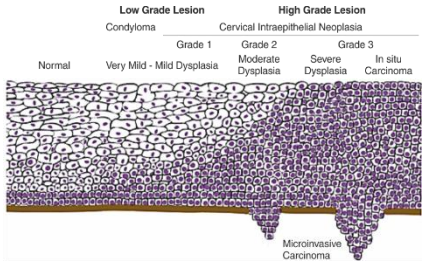


: $H^+$ : $Acetate^-$

: gap junctions, inactive in CIN

: tight junctions, loose in CIN

: ion buffers

: pumping mechanisms

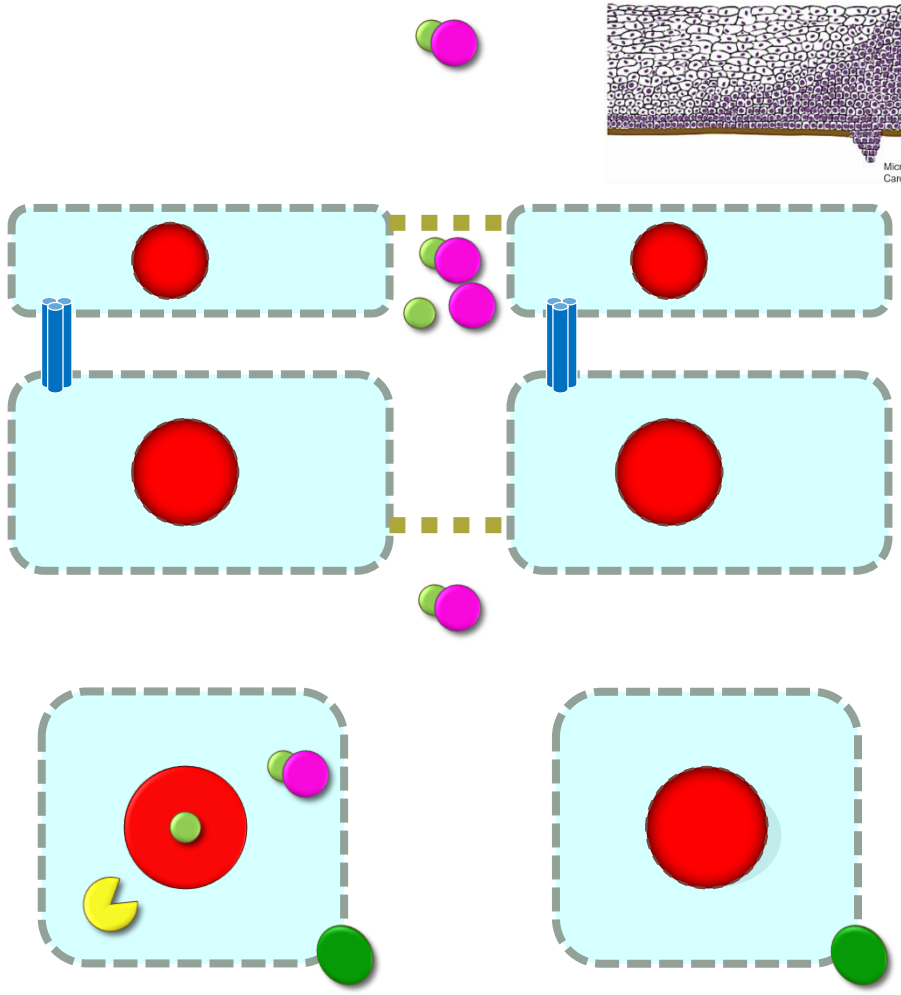

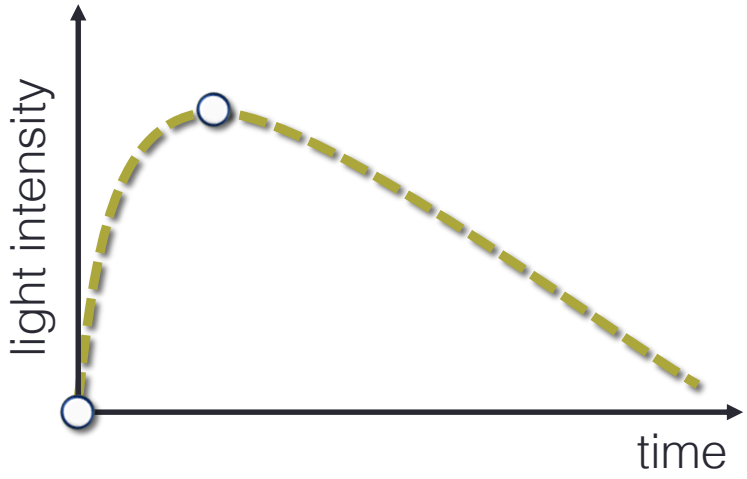


Balas C., Papoutsoglou G., Potirakis A., *IEEE JSTQE*, 2008

# Optical properties of normal and atypical tissue

## Normal epithelium is transparent

- Forward (Mie) scattering
  - Nucleus
  - Cell
- Fresnel reflection
- **Backscattering/Absorption**
  - Stroma
  - Vasculature

the “ouzo effect”

## Atypical, acetic acid-treated epithelium acts as a diffuser

- Strong backscattering

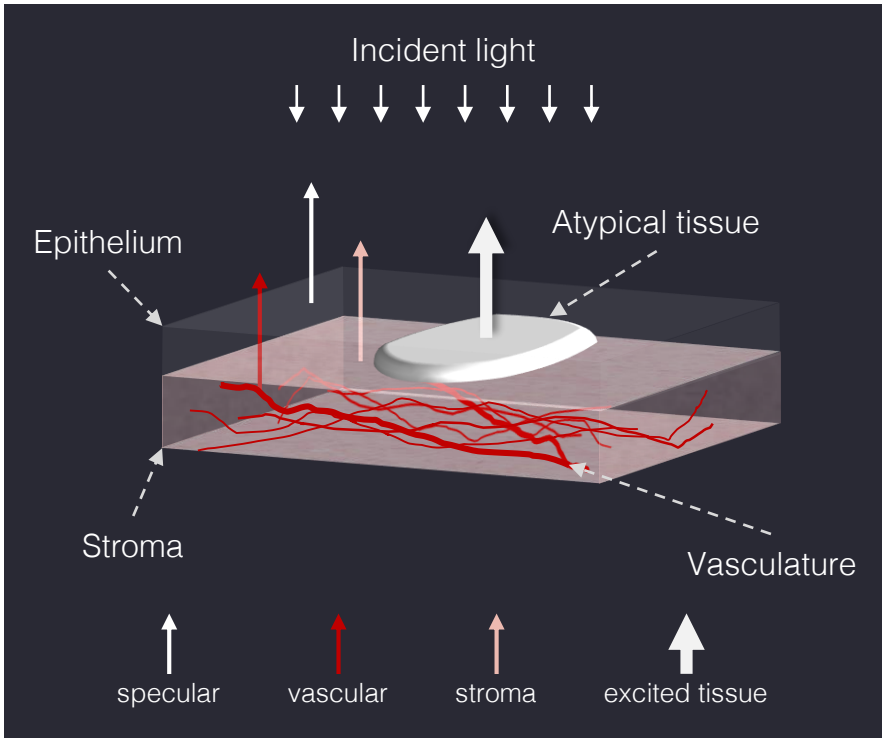


The backscattered photon increase accrues to small-sized-AA-induced cellular components in the cytoplasm and the nucleus. (Wu, et al., Optics Express,2005)

# Result 1: The origin of the bio-optical phenomenon

- **Road to acetowhitening:**
  - ionization (pH drop)
  - protein denaturation
  - cytoplasmic component coagulation

  } μs/ns regime (Finkelstein, *Phys. Life. Rev.*, 2004) << 4mins

  - change in the refractive index of the cell
  - alteration in the light scattering characteristics of the tissue
  - acetowhitening!

**The phenomenon's dynamics are not determined by the intrinsic time characteristics of the conformational changes, but from the dynamic characteristics of the change causing factor instead.**

**The development of a biophysical model of the biomarker kinetics allows for the quantitative assessment of several biological parameters that are determining the features of the experimental data.**

Conceptualization

Model development

Sensitivity Analysis

Solve the inverse

Parameter mapping

# THESIS RESULTS & CONTRIBUTIONS

## 2. MATHEMATICAL FRAMEWORK

- Differential equation system
- Model parameters
- Input-Output
- Preliminary validation

# Result 2: Model development and preliminary validation

- **Formulation of a coherent model of the system under study**

- **Validation**

  the biomarker kinetics and the effect's temporal characteristics are correlated with the histological features used to grade biopsy samples

- **Model-based fitting is possible**

**Relevant publications**

C. Balas, G. Papoutsoglou, C. Loukas, Y. Skiadas, C. Pappas, D. Haidopoulos, E. Diakomanolis, and W. P. Soutter, "*In vivo assessment of microstructural and functional alterations in cervical neoplasia*," in Conference proceedings: European Conferences on Biomedical Optics (ECBO), 2009.

# Model building strategy

## Conceptualization

- Modeling purpose
- Assumptions (aggregations, idealizations, etc.)

- **Mathematical framework**
  - Input-output parameter/variable relationship
  - bio-chemical/physical laws
- **Parameter identifiability**
  - Model reduction
  - Model restructuring
- **Parameter estimation**

## Validation

An integral component of the modeling process, being firmly embedded within all its stages rather than merely being an activity carried out once model identification has been completed

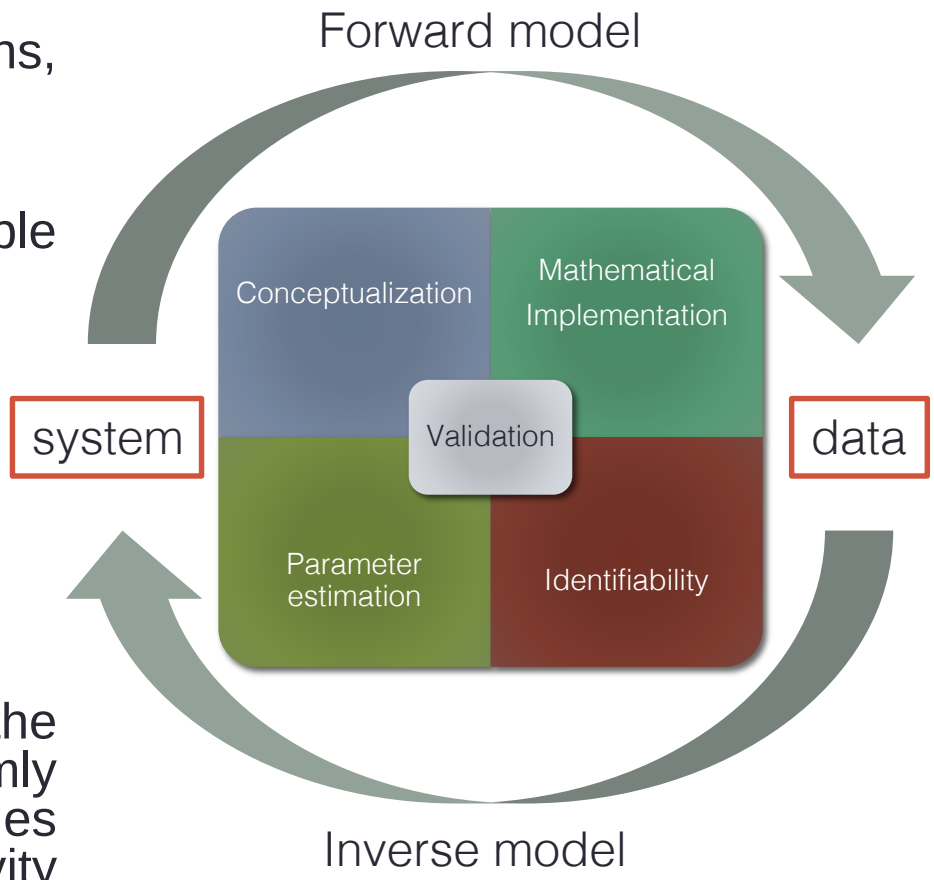

# Mathematical framework

We assume that each individual cell constitutes a two-compartmental system

1st compartment: cell (IS)

2nd compartment: extracellular space (ES)

buffered, well-stirred, kinetically homogeneous

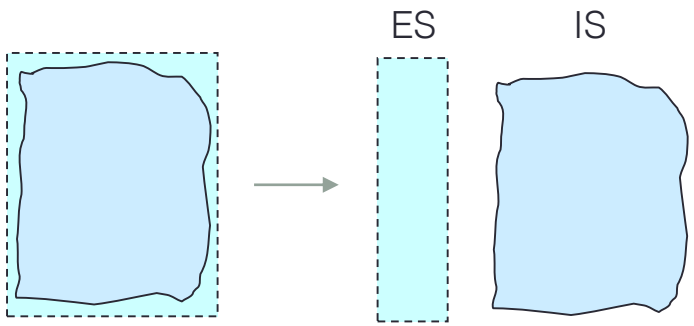


- Uniform distribution of cells
- CIN progression is proportional to the number of layers

stack of two-compartmental cell systems

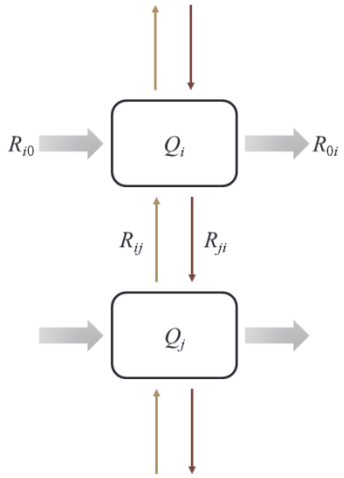


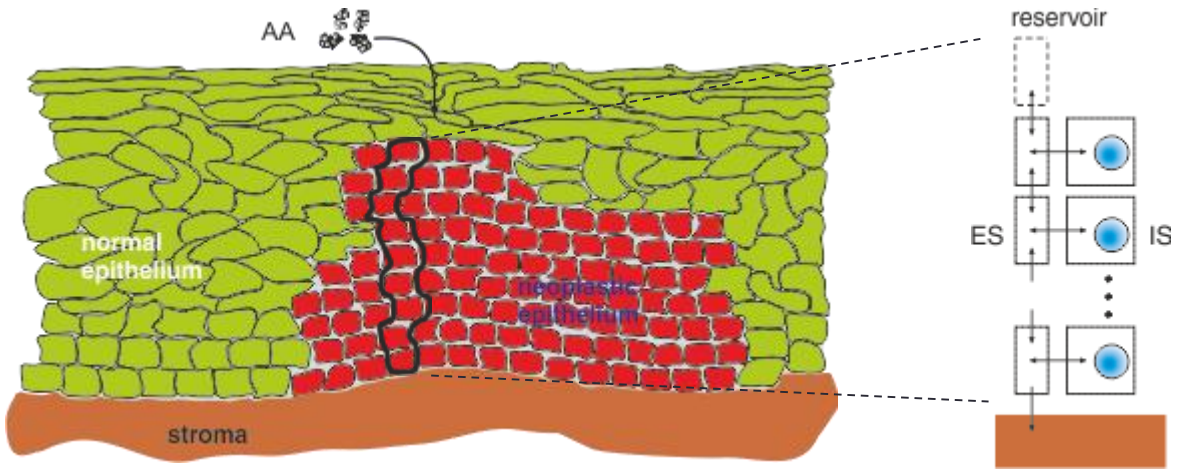

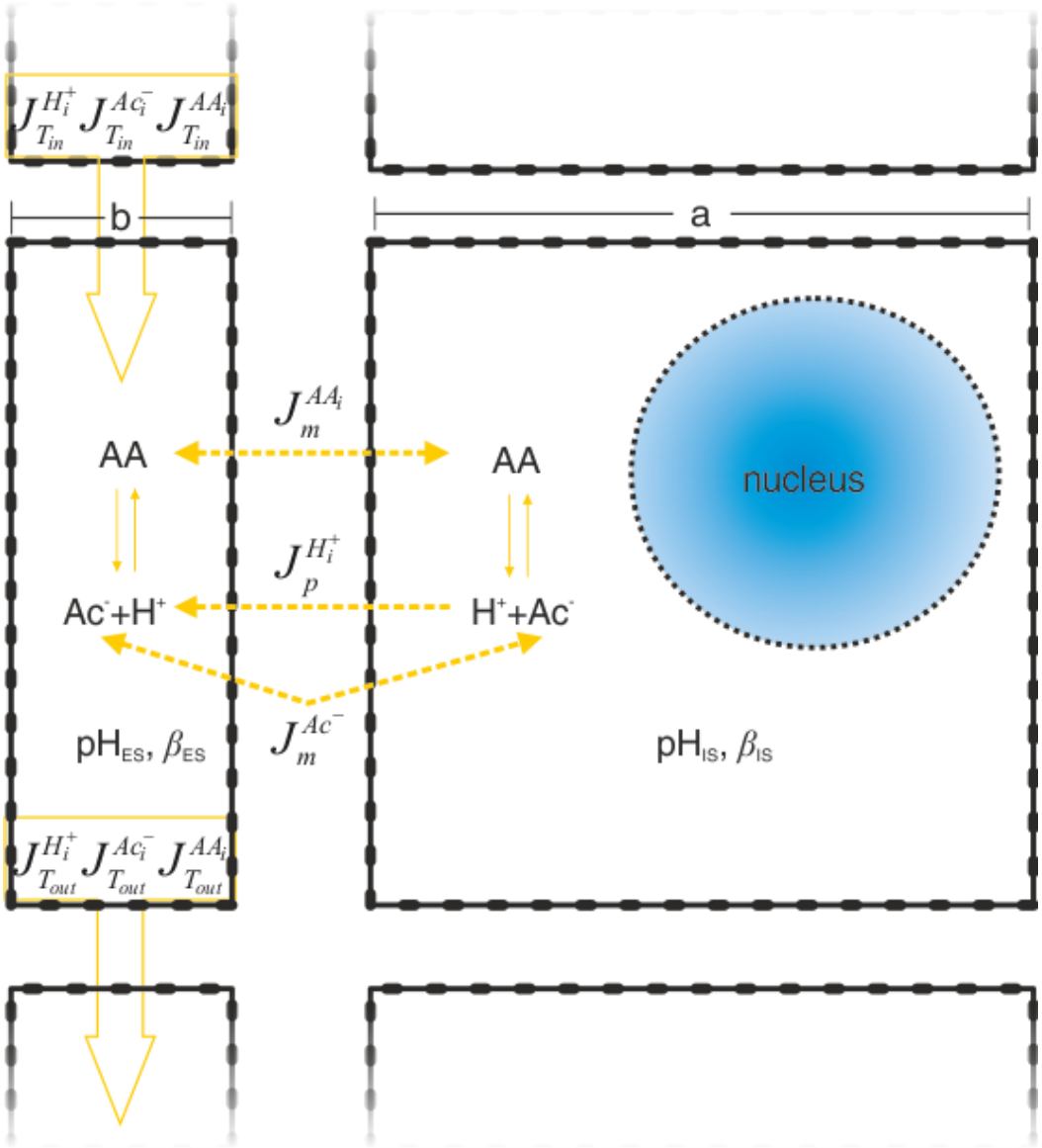


Layer i-1

Layer i

Layer i+1

i = 1 … #layers

# Differential equation system

## Intracellular Space

$$\dot{[TA]}^{i}_{IS} = \rho_{IS}\left(J_m^{AA_i} + J_m^{Ac_i}\right)$$

$$\dot{[H]}^{i}_{IS} = -\ln 10^{[H]^{i}_{IS}}\,\rho_{IS}\left(\beta_{IS}\right)^{-1}\left(\varphi^{i}_{IS} J_m^{AA_i} - \omega^{i}_{IS} J_m^{Ac_i} - J_p^{H_i}\right)$$

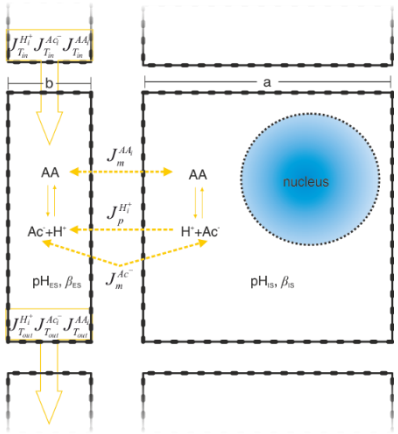


## Extracellular Space

$$\dot{[TA]}^{i}_{ES} = \rho_{ES}\left(J_m^{AA_i} + J_m^{Ac_i}\right) + \rho_{TJ} g_{TJ}\left(J_{TJ}^{AA_{i-1}} - J_{TJ}^{AA_{i+1}} + J_{TJ}^{Ac_{i-1}} - J_{TJ}^{Ac_{i+1}}\right)$$

$$\dot{[H]}^{i}_{ES} = -\ln 10^{[H]^{i}_{ES}}\left(\beta_{ES}\right)^{-1}\left\{\rho_{ES}\left(\varphi^{i}_{ES} J_m^{AA_i} - \omega^{i}_{ES} J_m^{Ac_i} - J_p^{H_i}\right) + \right.$$

$$\left. + \rho_{TJ} g_{TJ}\left[\varphi^{i}_{ES}\left(J_{TJ}^{AA_{i-1}} - J_{TJ}^{AA_{i+1}}\right) + \omega^{i}_{ES}\left(J_{TJ}^{Ac_{i-1}} - J_{TJ}^{Ac_{i+1}}\right)\right]\right\}$$

Reservoir layer: no IS

Last layer: $J_{TJ}^{[S]_{i+1}} \rightarrow K_V [S]$

Fick: $J^{(S)}_{I\rightarrow II} = P^{(S)}\left([S]^{I} - [S]^{II}\right)$

GHK: $J^{(S)}_{I\rightarrow II} = \dfrac{z_S F V_m}{RT\left(1 - e^{-z_S F V_m/RT}\right)} P^{(S)}\left([S]^{I} - [S]^{II} e^{-z_S F V_m/RT}\right)$

# Mathematical particularities

- **adaptable structure**
  - the number of layers **defines** the number of differential equations that are integrated in the system.
- **dynamic degree of ionization of AA ($\omega$, $\phi$)**

$$\omega_{IS}^{i} = \frac{K_{\alpha}}{[H]_{IS}^{i} + K_{\alpha} + 2.3(\beta_{IS})^{-1} K_{\alpha} \frac{[H]_{IS}^{i}}{[H]_{IS}^{i} + K_{\alpha}} [TA]_{IS}^{i}}$$

- **trans-layer voltage ($\Delta V_{TJ}$)**

$$\Delta V_{TJ} = \frac{RT}{F} \ln \frac{P_{TJ}^{(H)} [H]_{ES}^{i-1} + P_{TJ}^{(Ac)} [Ac]_{ES}^{i}}{P_{TJ}^{(H)} [H]_{ES}^{i} + P_{TJ}^{(Ac)} [Ac]_{ES}^{i-1}}$$

- **proton pumping rate**

$$J_p(pH_{IS}) = \begin{cases} \frac{K_p}{pH_{IS,K_p} - 7.4} pH_{IS}, & pH_{IS} > pH_{IS,K_p} \\ K_p, & pH_{IS} = pH_{IS,K_p} \\ \frac{K_p}{pH_{IS,K_p} - 6} pH_{IS}, & pH_{IS} < pH_{IS,K_p} \end{cases}$$

- **[H] to pH conversion**

$$\frac{d[H]^{IS}}{dt} = -\frac{2.303}{\beta_{IS}} [H]^{IS} \frac{(dQ_H)^{IS}}{dt}$$

**Model: multi-resolution design**

- no single analytical representation
- model equations are not factorable or/and cannot anyhow be algebraically manipulative

# Model biological parameters

| | Parameter | Epexegesis |
|---|---|---|
| Structural | $a^3$ | volume (in μm$^3$) of the IS – $V_{IS}$ |
| | $a^2 \times b$ | volume (in μm$^3$) of the ES – $V_{ES}$ |
| | $a^2$ | cell diffusion area (in μm$^2$) – $A_m$ |
| | $a \times b$ | TJ diffusion area (in μm$^2$) – $A_{TJ}$ |
| | $N$ | number of epithelial neoplastic layers |
| Functional | $\beta_{IS}$ | IS intrinsic buffering capacity |
| | $\beta_{ES}$ | ES intrinsic buffering capacity |
| | $pH_{IS}$ | IS pH |
| | $pH_{ES}$ | ES pH |
| | $pH_{IS,Kp}$ | pH level in which the $H^+$ pump activity maximizes |
| | $g_{TJ}$ | TJ porosity factor |
| | $K_V$ | solute diffusion rate at the tissue-stroma interface |
| | $P^{(S)}$ | solute permeabilities |
| | $\Delta V_{TJ}, \Delta V_m$ | transmembrane voltage gradient (TJ and cell's membrane) |

# Input-output

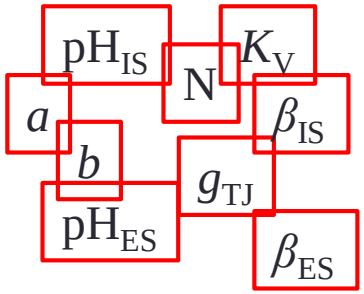


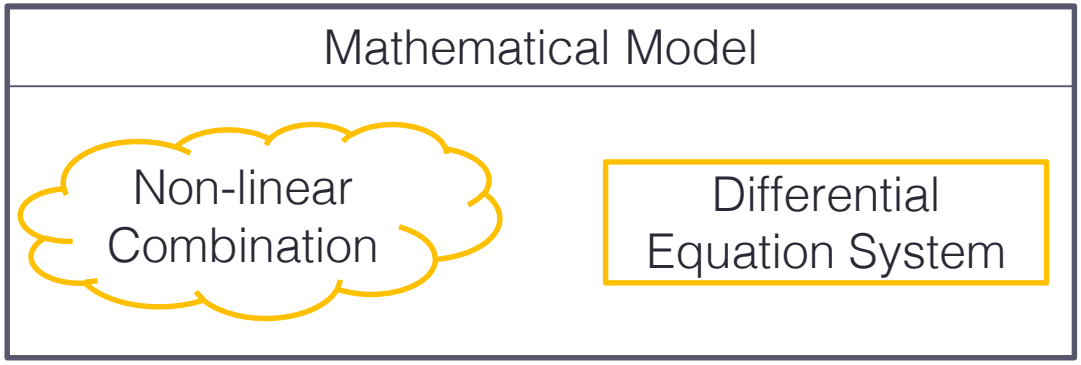


the intracellular $H^+$ concentration vs. time curve is the model's output

$$y^{M}(t) = \sum_{i=1}^{N} \left\{ [H]_{IS}^{i}(t) - [H]_{IS}^{i}(0) \right\}$$

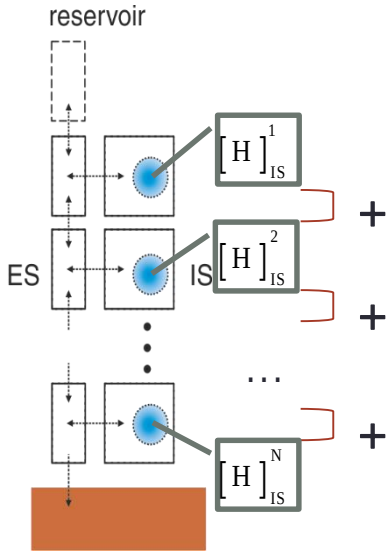


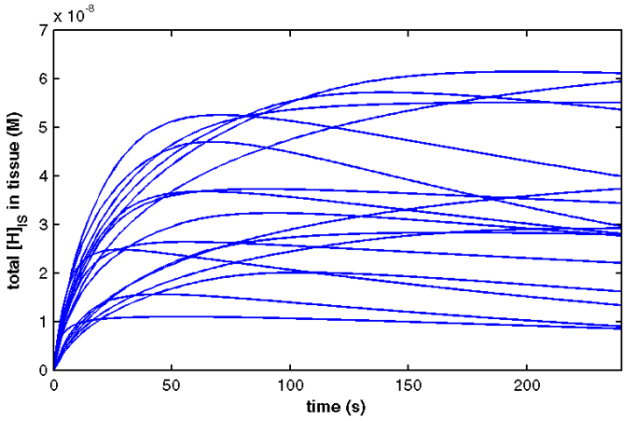

# Result 2: Preliminary validation of the developed model

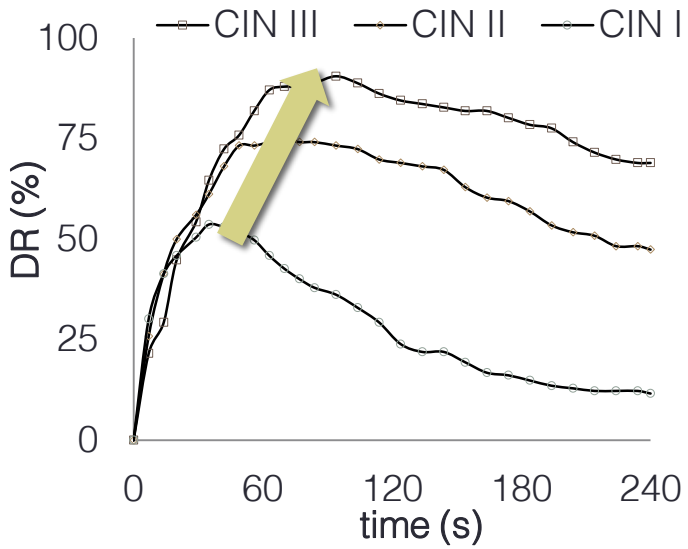


- the biomarker kinetics and the AW characteristics are correlated with the histological features used to grade biopsy samples

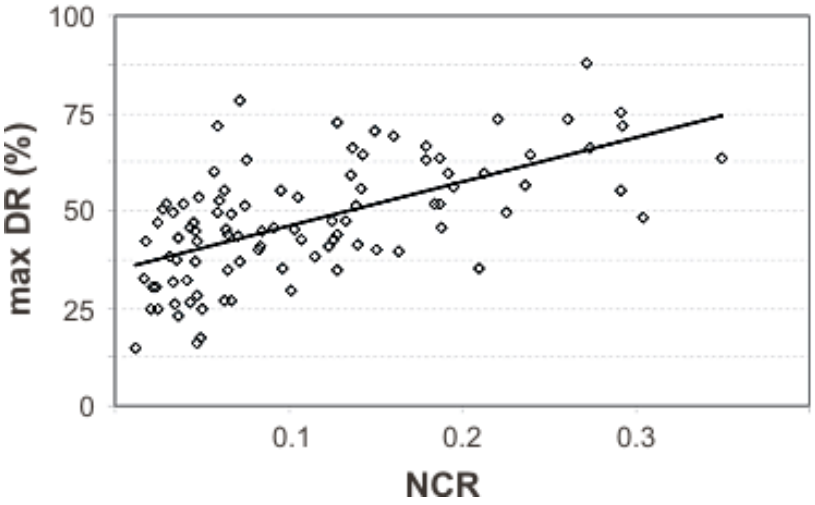


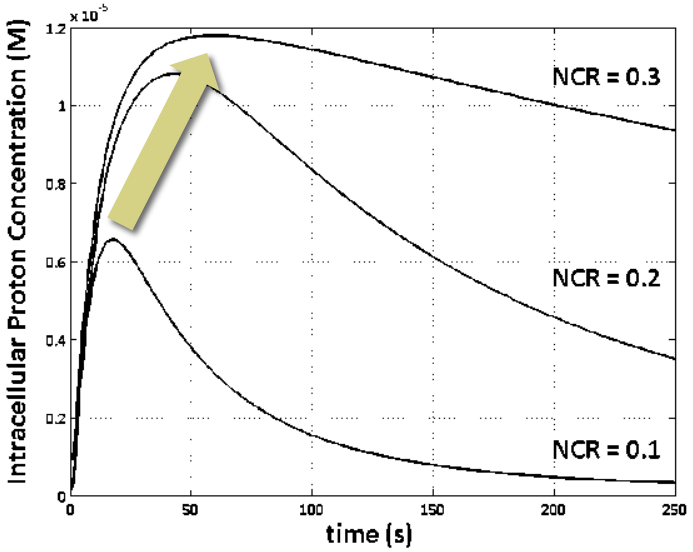


Balas C., Papoutsoglou G., *et al.*, *EMBO*, 2009

# Result 2: Model development and preliminary validation

- **Neoplasia development imposes a series of structural and functional alterations**
- **Clear correlation between the dynamic scattering characteristics of the optical effect and model predictions**
- **Model-based fitting is possible**
  - calculation of dynamic optical parameters that correlate well with histological features used to grade biopsy samples

Conceptualization
Mathematical Implementation
Sensitivity Analysis
Solve the inverse
Parameter mapping

# THESIS RESULTS & CONTRIBUTIONS

## 3. SENSITIVITY ANALYSIS

Model reduction

Validation

Model restructuring

# Result 3: Critical, neoplasia-related parameters

- **Parameter reduction**
  - $K_V$: null TOS function
  - $\beta_{IS}$, $\beta_{ES}$, $pH_{IS}$, $a$: not fulfilling the combined identification criteria
- **key determinants of the model's output**
  - Structural: N, $b$ that relate to histology grading
  - Functional: $pH_{ES}$, $g_{TJ}$ that relate to the altered tissue activity

FOS: $S_i = V_i / V(Y)$

TOS: $S_{Ti} = S_i + S_{ij} + \ldots + S_{ij..k}$

**Relevant publications**


1. G. Papoutsoglou, A. Anastasopoulou, G. Stavrakakis, P. Soutter, and C. Balas, "*In vivo dynamic imaging, in silico modeling and global sensitivity analysis for the study and the diagnosis of epithelial neoplasia.*," in Conference proceedings : Annual International Conference of the IEEE Engineering in Medicine and Biology Society. Boston, USA, 2011, vol. 2011, pp. 95–9
2. G. S. Papoutsoglou and C. Balas, "*Estimation of neoplasia-related biological parameters through modeling and sensitivity analysis of optical molecular imaging data.*," IEEE Transactions on Biomedical Engineering, vol. 60, no. 5, pp. 1241–9, May 2013.

# Preliminary global sensitivity analysis results

FOS and TOS depend

- Model's structure
- Probability density function assumed for each input factor
- Parameter value ranges

- **Preliminary study**
  - Uniform distributions
  - Largest possible value ranges for the input parameters

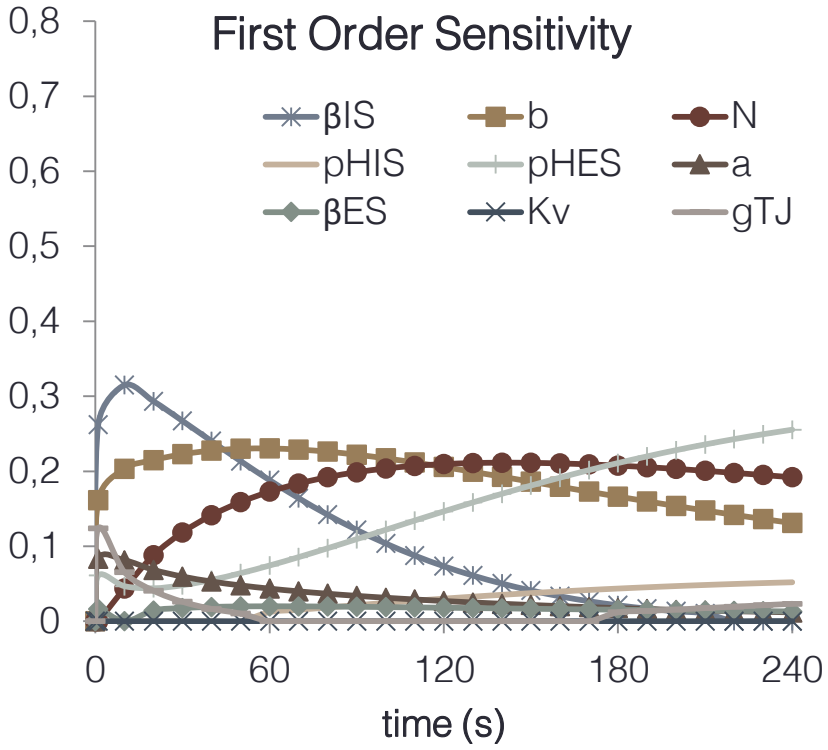


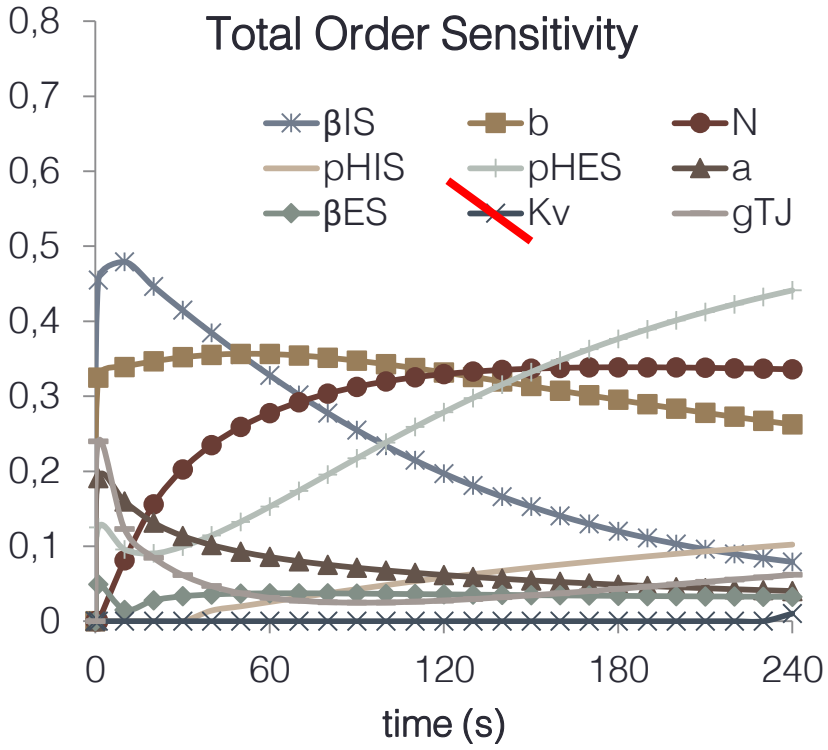


Papoutsoglou G., Anastasopoulou A., Stavrakakis G., Scouter P., Balas C. *IEEE EMBC*, 2011

# Parameter ranking

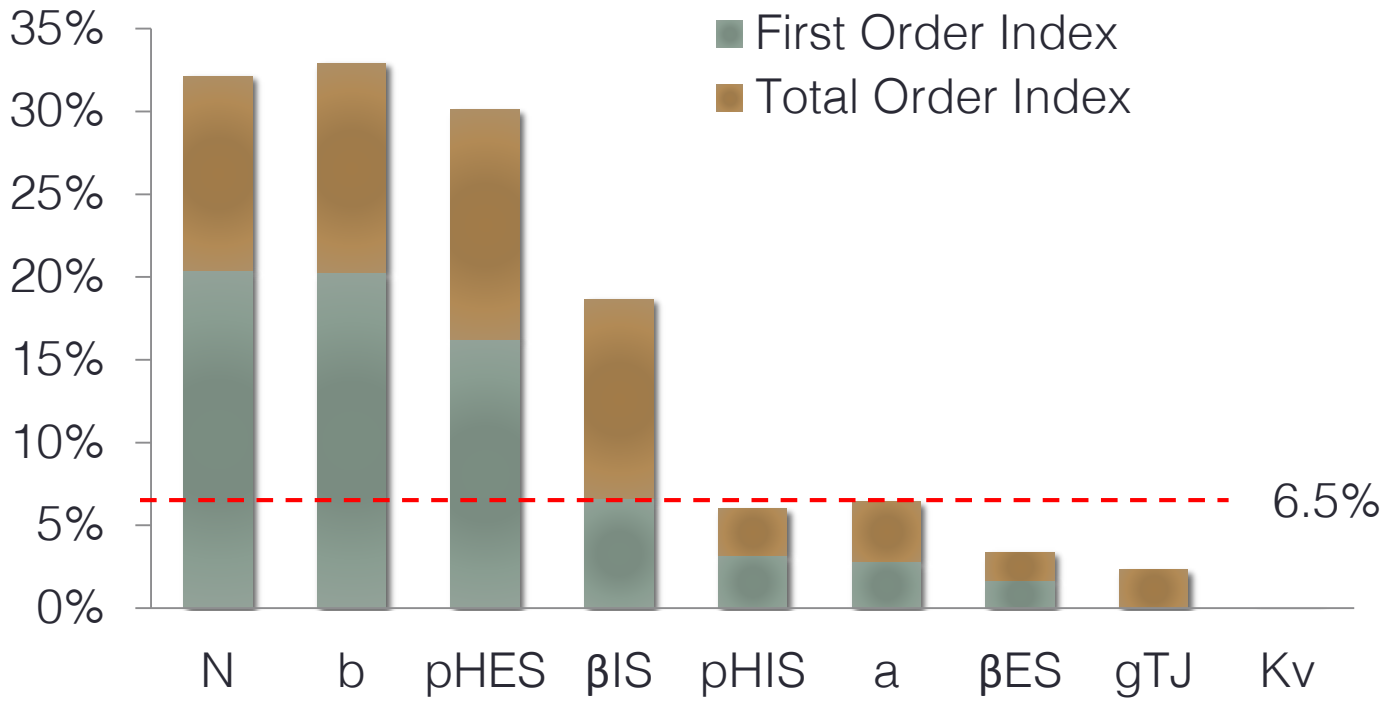


- N: histology grading parameter
- *b:* increases with neoplasia progression (Walker, et al., *Physiol. Meas.*, 2003)
- $pH_{ES}$: precursor of invasive cells (Gatenby, et. al., *Cancer Res.*,2006)
- $\beta_{IS}$: cell's dominant suppressor of the acute increase in intracellular $H^+$
- Total index of the rest of the parameters was less than 6.5% suggesting a negligible effect on the model's output

# Correspondence with experimental data

- Neoplasia grade is highly correlated with the number of dysplastic layers (N)
  - N can be assessed in a semi-quantitative manner from biopsy samples
- 30 experimental curves (biopsy confirmed)
  - 10 CIN I (low grade) and
  - 20 CIN II, III (high grade)

- At t=142s where the importance of N maximizes the change of the median reflectance value is **1.25 times**
- Suggests a correspondence between theoretical predictions and experimental data

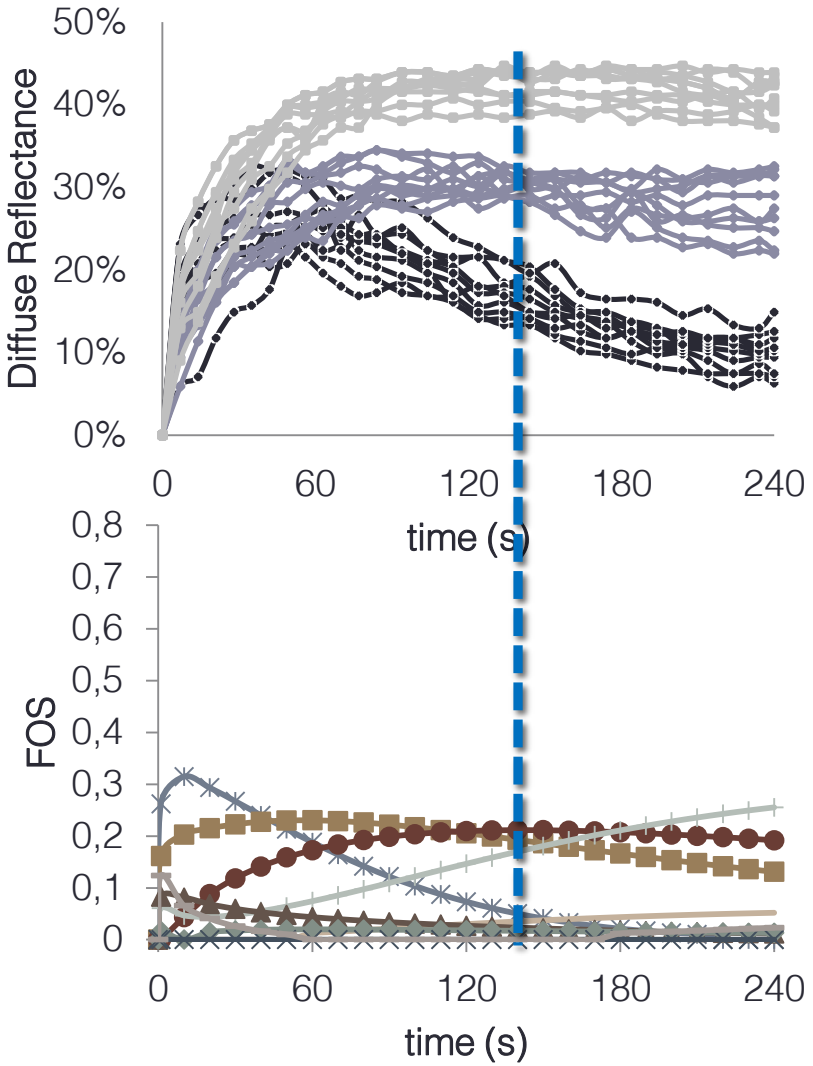

# Revisited global sensitivity analysis

- Parameter distributions
  - Thorough literature study
    - Uniform: N, $\beta_{ES}$, $\beta_{IS}$, $pH_{ES}$, $pH_{IS}$, $a$
    - Triangular: $b$, $K_V$
    - Log-triangular: $g_{TJ}$
- Corrected parameter values
- Model update

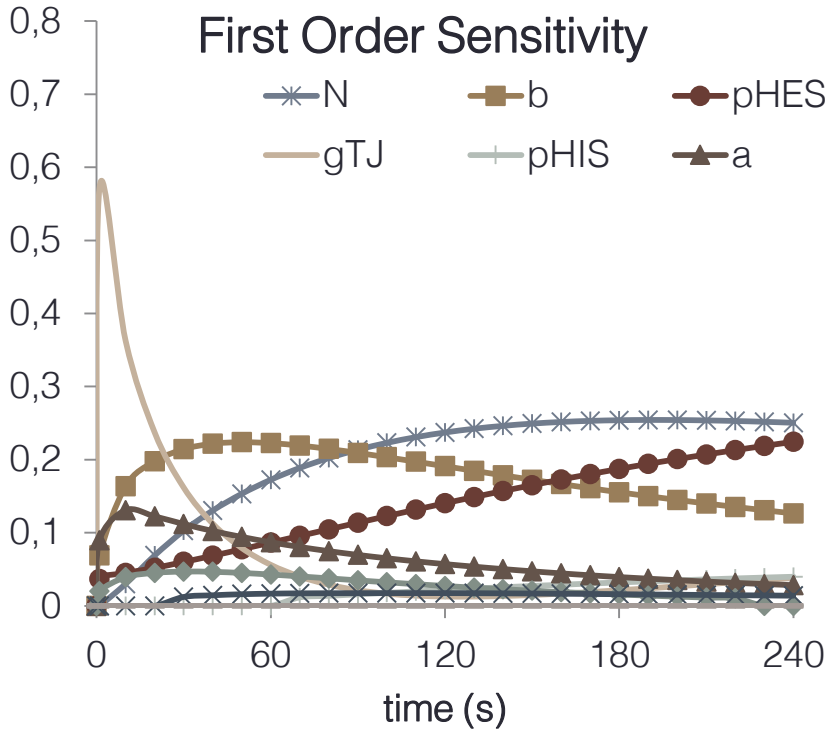


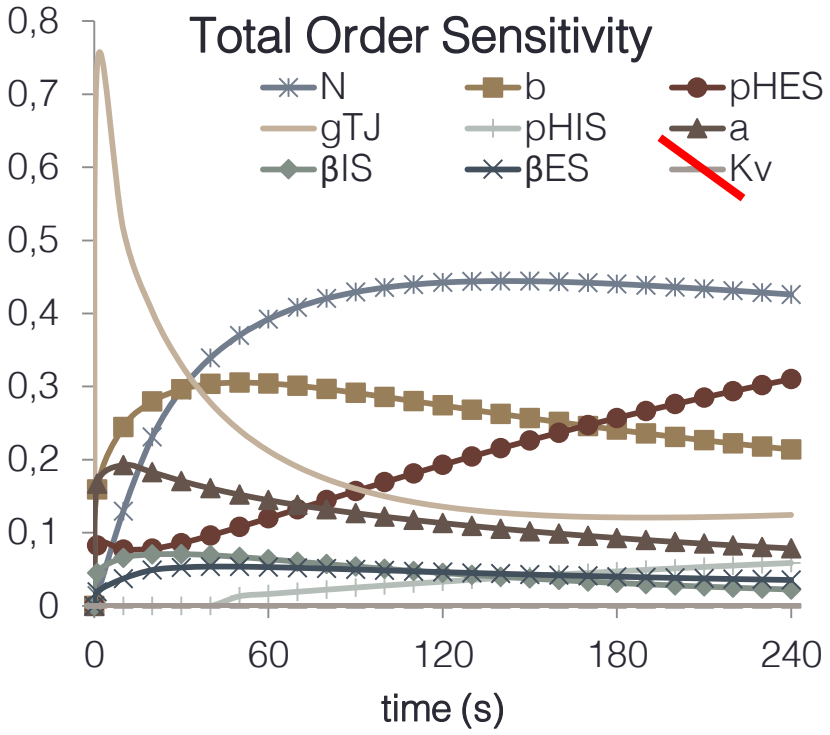


Papoutsoglou G., Balas C., *IEEE TBME,* 2013

# Parameter ranking (revisited)

## descending mean FOS index

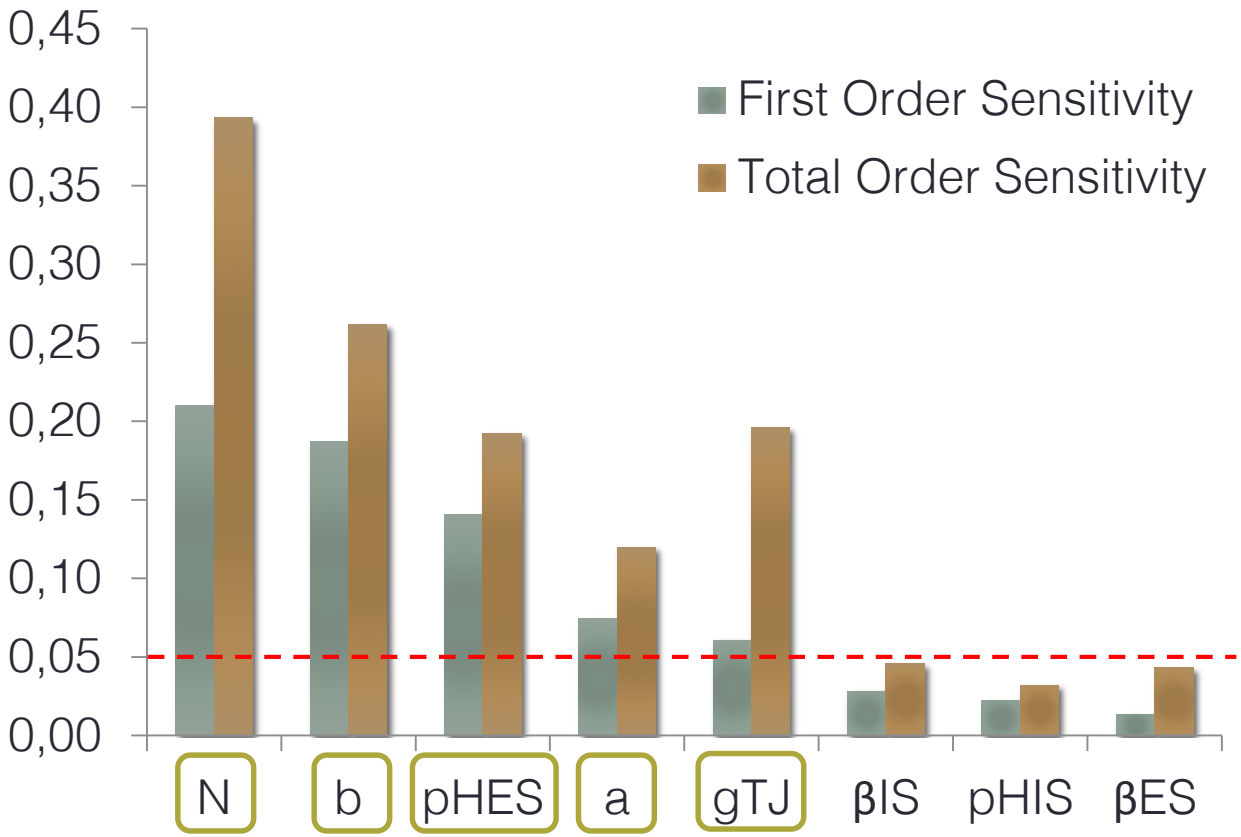


The influence of the rest of the parameters was less than 5% suggesting a negligible effect on the model's output

# Parameter collinearities

$$\mathbf{S}_D = \begin{bmatrix} S_{T_1}|_{t_1} & \cdots & S_{T_k}|_{t_1} \\ \vdots & \ddots & \vdots \\ S_{T_1}|_{t_s} & \cdots & S_{T_k}|_{t_s} \end{bmatrix}$$

Pearson's r

| | | | | | | | | |
|---|---|---|---|---|---|---|---|---|
| $a$ | **1** | 0,58 | 0,44 | **0.95 (1)** | -0,73 | -0,90 | -0,93 | 0,87 |
| $b$ | 0,58 | **1** | **0.96 (1)** | 0,76 | 0,12 | -0,53 | -0,51 | 0,12 |
| $\beta_{ES}$ | 0,44 | **0.96 (1)** | **1** | 0,67 | 0,24 | -0,44 | -0,41 | -0,03 |
| $\beta_{IS}$ | **0.95 (1)** | 0,76 | 0,67 | **1** | -0,55 | -0,93 | -0,93 | 0,68 |
| $N$ | -0,73 | 0,12 | 0,24 | -0,55 | **1** | 0,72 | 0,77 | -0,93 |
| $pH_{ES}$ | -0,90 | -0,53 | -0,44 | -0,93 | 0,72 | **1** | **0.99 (1)** | -0,73 |
| $pH_{IS}$ | -0,93 | -0,51 | -0,41 | -0,93 | 0,77 | **0.99 (1)** | **1** | -0,79 |
| $g_{TJ}$ | 0,87 | 0,12 | -0,03 | 0,68 | -0,93 | -0,73 | -0,79 | **1** |
| | $a$ | $b$ | $\beta_{ES}$ | $\beta_{IS}$ | $N$ | $pH_{ES}$ | $pH_{IS}$ | $g_{TJ}$ |

Full set

Reduced set

| | | | | | |
|---|---|---|---|---|---|
| **1** | 0,60 | -0,80 | -0,87 | 0,9 | $a$ |
| 0,60 | **1** | -0,02 | -0,66 | 0,19 | $b$ |
| -0,80 | -0,02 | **1** | 0,68 | -0,94 | $N$ |
| 0,87 | -0,66 | 0,68 | **1** | -0,67 | $pH_{ES}$ |
| 0,9 | 0,19 | -0,94 | -0,67 | **1** | $g_{TJ}$ |
| $a$ | $b$ | $N$ | $pH_{ES}$ | $g_{TJ}$ | |

| | | | | | |
|---|---|---|---|---|---|
| 1 | 1 | 1 | 1 | 1 | 1 |
| 0,95-1 | 0,9 - 0,94 | 0,7 - 0,89 | 0,4 - 0,69 | 0,1 - 0,39 | 0 - 0,09 |

- Repeatedly remove one unidentifiable parameter each time (r>0.95)
- Choose according to disease specific importance

# Estimability Analysis

## Parameter interdependencies

$$\mathrm{ER}(t) = S_i(t) \Big/ \sum_{j=1}^{k} S_{T_j}(t)$$

- Similar to the FOS ranking
- high ranking of $g_{\mathrm{TJ}}$: high FOS index at first time instances

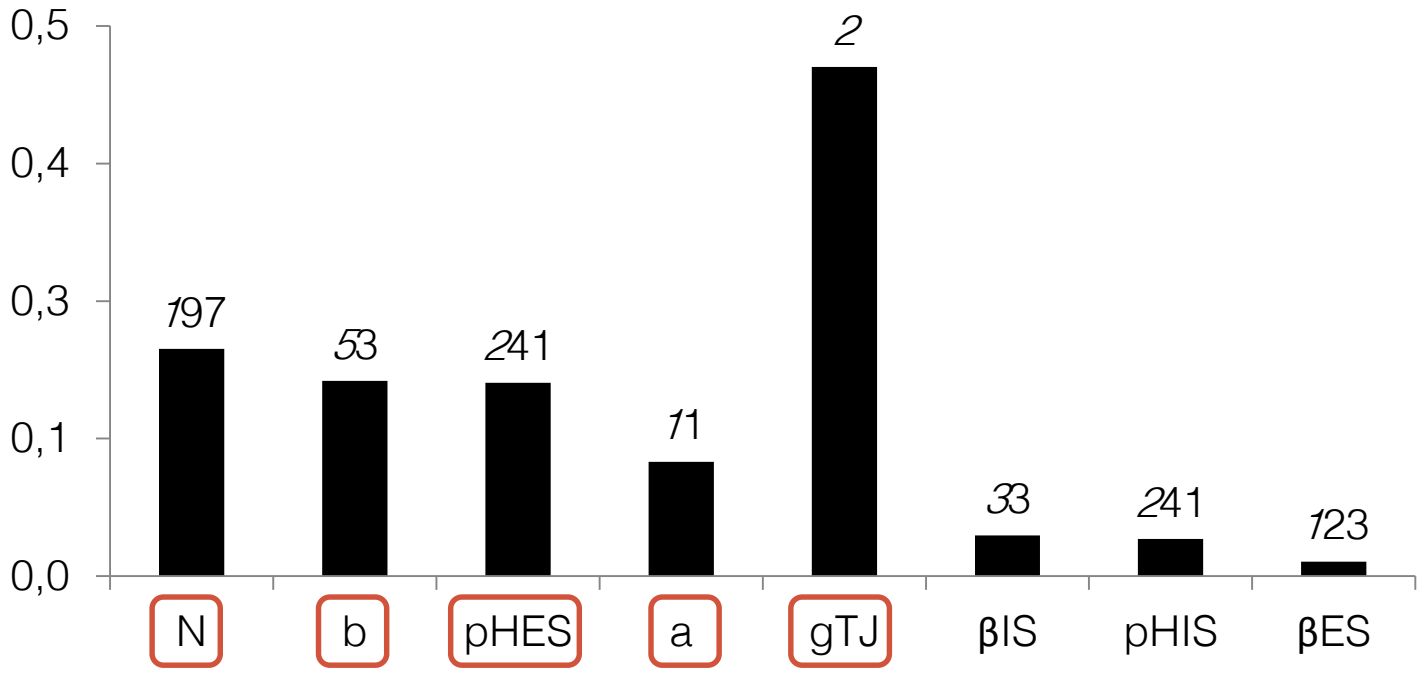

# High level validation of the dimensionality reduction

- 30 NDR vs. time experimental curves
  - 10 CIN I (LG), 10 CIN II and 10 CIN II (HG)
- fitting by comparison with 20.000 normalized [$H^+$] vs. time curves (GSA)
  - not unique set of parameter combinations
  - fit each experimental curve with ten, best fitting model curves ($R^2$>93%)
  - assign 100 curves to each CIN class

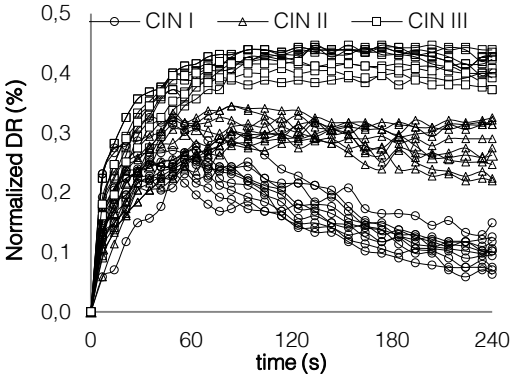


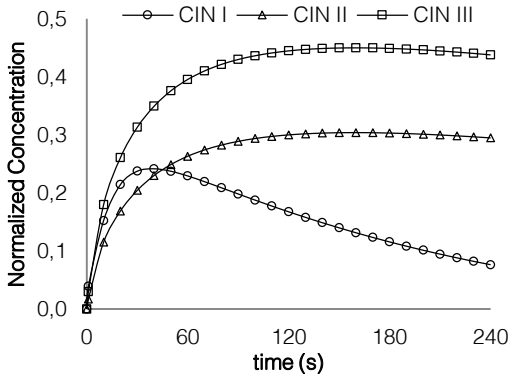


This has shown for the first time that the solution of the inverse problem can be possible

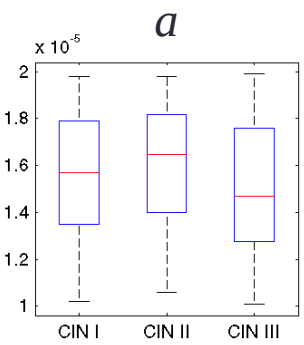


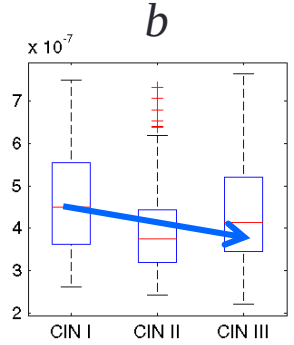


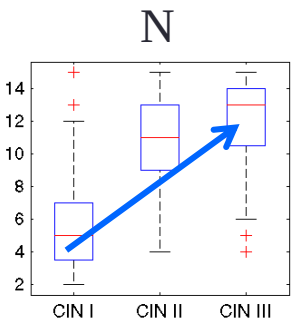


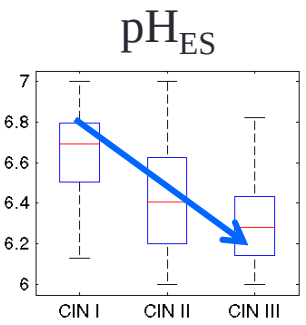


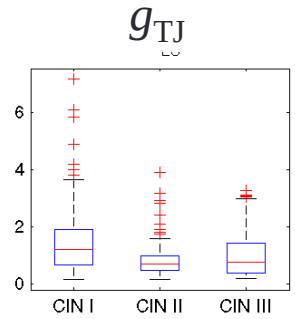

# Model restructuring (1)

- **dynamic range of *b***
  - significant histology parameter
  - high overlapping of the estimated values
- **remodel parameter $g_{TJ}$**
  - high collinearity with N

Full set

| | $N$ | $b$ | $pH_{ES}$ | $g_{TJ}$ | $\beta_{IS}$ | $pH_{IS}$ | $\beta_{ES}$ | $a$ |
|---|---|---|---|---|---|---|---|---|
| $N$ | 1 | 0,25 | 0,55 | -0,91 | -0,56 | 0,79 | 0,51 | -0,83 |
| $b$ | 0,25 | 1 | -0,44 | 0,13 | 0,65 | -0,27 | 0,92 | 0,28 |
| $pH_{ES}$ | 0,55 | -0,44 | 1 | -0,66 | -0,77 | 0,92 | -0,08 | -0,67 |
| $g_{TJ}$ | -0,91 | 0,13 | -0,66 | 1 | 0,84 | -0,88 | -0,17 | **0,99 (1)** |
| $\beta_{IS}$ | -0,56 | 0,65 | -0,77 | 0,84 | 1 | -0,84 | 0,37 | 0,91 |
| $pH_{IS}$ | 0,79 | -0,27 | 0,92 | -0,88 | -0,84 | 1 | 0,11 | -0,87 |
| $\beta_{ES}$ | 0,51 | 0,92 | -0,08 | -0,17 | 0,37 | 0,11 | 1 | -0,01 |
| $a$ | -0,83 | 0,28 | -0,67 | **0,99 (1)** | 0,91 | -0,87 | -0,01 | 1 |

*before restructuring*

| | $a$ | $b$ | $\beta_{ES}$ | $\beta_{IS}$ | $N$ | $pH_{ES}$ | $pH_{IS}$ | $g_{TJ}$ |
|---|---|---|---|---|---|---|---|---|
| $a$ | 1 | 0,58 | 0,44 | **0.95 (1)** | -0,73 | -0,90 | -0,93 | 0,87 |
| $b$ | 0,58 | 1 | **0.96 (1)** | 0,76 | 0,12 | -0,53 | -0,51 | 0,12 |
| $\beta_{ES}$ | 0,44 | **0.96 (1)** | 1 | 0,67 | 0,24 | -0,44 | -0,41 | -0,03 |
| $\beta_{IS}$ | **0.95 (1)** | 0,76 | 0,67 | 1 | -0,55 | -0,93 | -0,93 | 0,68 |
| $N$ | -0,73 | 0,12 | 0,24 | -0,55 | 1 | 0,72 | 0,77 | -0,93 |
| $pH_{ES}$ | -0,90 | -0,53 | -0,44 | -0,93 | 0,72 | 1 | **0.99 (1)** | -0,73 |
| $pH_{IS}$ | -0,93 | -0,51 | -0,41 | -0,93 | 0,77 | **0.99 (1)** | 1 | -0,79 |
| $g_{TJ}$ | 0,87 | 0,12 | -0,03 | 0,68 | -0,93 | -0,73 | -0,79 | 1 |

| | | | | | |
|---|---|---|---|---|---|
| 1 | 0,60 | -0,80 | -0,87 | 0,9 | $a$ |
| 0,60 | 1 | -0,02 | -0,66 | 0,19 | $b$ |
| -0,80 | -0,02 | 1 | 0,68 | -0,94 | $N$ |
| 0,87 | -0,66 | 0,68 | 1 | -0,67 | $pH_{ES}$ |
| 0,9 | 0,19 | -0,94 | -0,67 | 1 | $g_{TJ}$ |
| $a$ | $b$ | $N$ | $pH_{ES}$ | $g_{TJ}$ | |

Reduced set

| | | | | |
|---|---|---|---|---|
| 1 | -0,24 | -0,40 | -0,83 | $N$ |
| -0,24 | 1 | -0,49 | 0,72 | $b$ |
| -0,40 | -0,49 | 1 | 0,09 | $pH_{ES}$ |
| -0,83 | 0,72 | 0,09 | 1 | $g_{TJ}$ |
| $N$ | $b$ | $pH_{ES}$ | $g_{TJ}$ | |

# Model restructuring (2)

- **alleviate parameter $a$**
  - within the highest ranked ones
    - lowest ranked
    - smallest ER
    - high collinearities with the rest of the parameters (negative effect on the identifiability of these parameters)
  - lowest correlation with neoplasia development according to model assumptions

# Result 3: Critical, neoplasia-related parameters

## Systematic parameter reduction

- $K_V$: null TOS function
- $\beta_{IS}$, $\beta_{ES}$, $pH_{IS}$: close to unity correlation coefficient + low ER + low FOS
- $a$: high collinearity with the highest ranked parameters

**key determinants of the measurable/modeled dynamic optical characteristics**

- N, $b$ are the key parameters onto which routine histological grading of biopsies is based
- $pH_{ES}$ is strongly linked with the ability of tumor cells to form invasive cancers
- $g_{TJ}$ represents the tight junction functional changes due to malfunction at precancers

**Concurrent estimation and for every spatial point of the tissue is possible through optical measurements.**

**Ideally, diagnosis and prediction can be performed at the same consultation and non-invasively**

# THESIS RESULTS & CONTRIBUTIONS

# 4. SOLUTION OF THE INVERSE PROBLEM

Problem statement

In silico experimental setup

Results

# Result 4: Solution of the inverse problem

- **We quantitated the overall quality of the solutions to the inverse problem**
  - Aggregate error < 5%
- **Estimation of the four most important biological parameters, is possible with highly accuracy and reproducibility using DE or CRSwCH methods**
  - Aggregate error ~1%

**Relevant publications**

1. Papoutsoglou G., Stamatiadou M., Stavrakakis G., Balas C., "*In vivo Estimation of Functional and Structural Characteristics in Epithelial Neoplasia*", OSA Optical Molecular Probes, Imaging and Drug Delivery (OMP), Monterey, California, USA, April 4, 2011
2. G. Papoutsoglou, M. Stamatiadou, and C. Balas, "*In silico Modeling and Global Optimization of Dynamic Bio-optical Processes for Probing, in vivo, Biological Features of Neoplasia*," IEEE iCBEB, Macau, China, 2012

# Employed global optimizers

- **no guarantee of optimality**
  1. find sets of solutions by several dissimilar methods
  2. decide the degree of convergence that is actually achieved
- **Deterministic**
  - gblSolve
- **Stochastic**
  - Controlled Random Search with Competing Heuristics (CRSwCH)
  - Differential Evolution (DE)
  - Shuffled Complex Evolution (SCE)
  - Particle Swarm Optimization (PSO)
  - ThermoDynamically Adaptive Simulated Annealing (tdASA)
  - Stochastic Ranking Evolutionary Strategy (SRES)
  - Mixed-Integer Dynamic Ant Colony Optimization (MIDACO)

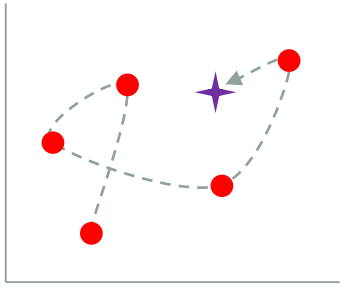

Point to Point

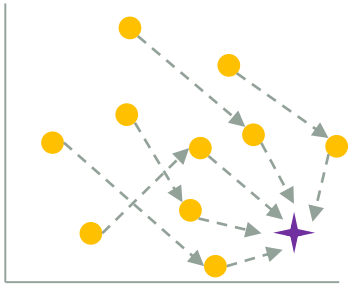

Population based

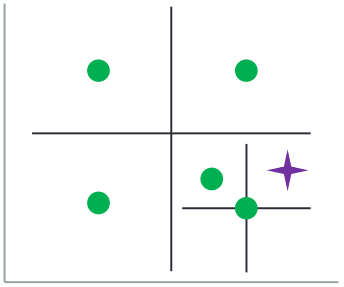

Bound division

# Derivative-free parameter estimation

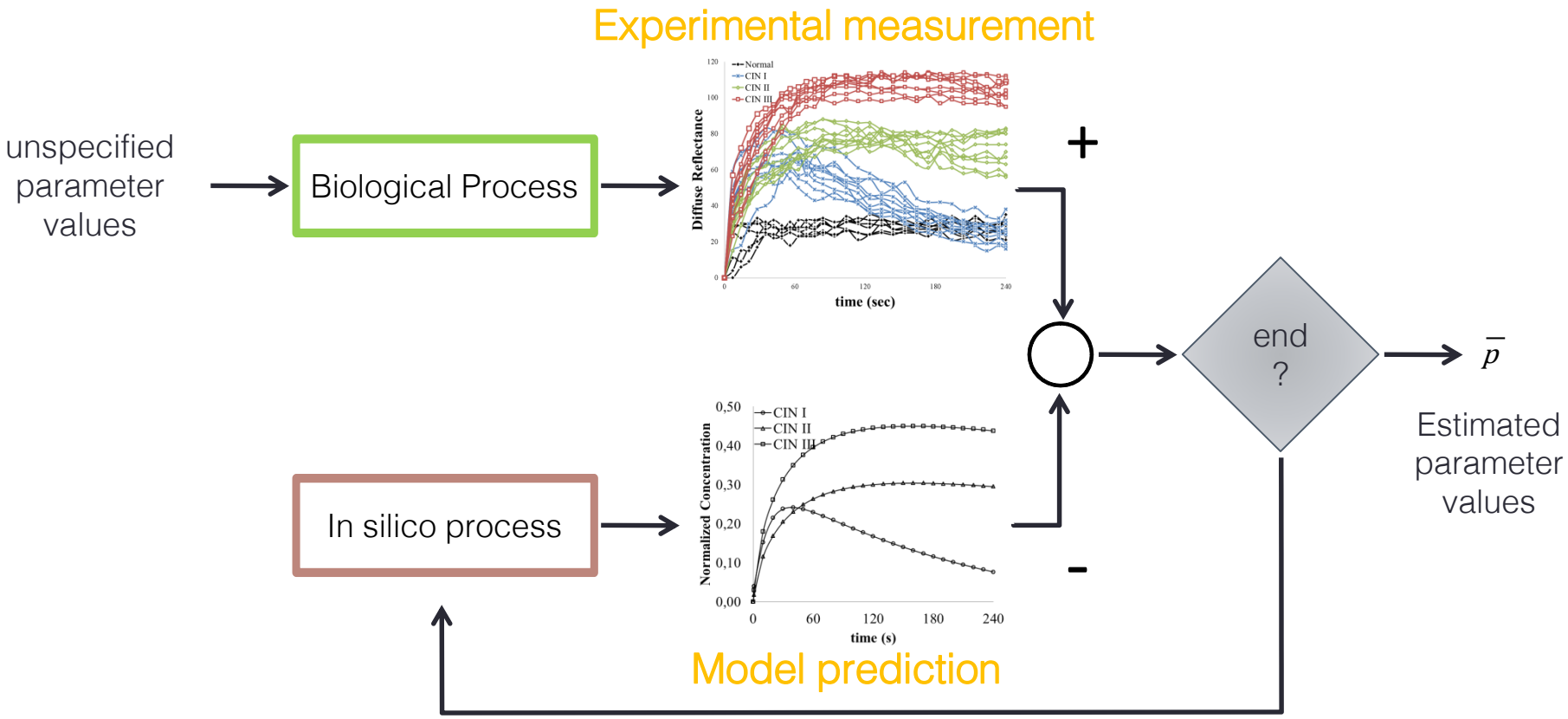

# Problem statement

minimize $J = \left\| y^{\exp}\ \mathbf{p}, t\ - y^{\mathrm{M}}\ \bar{\mathbf{p}}, t\ \right\|,$

subject to $f\left(\frac{d\mathbf{x}}{dt}, \mathbf{x}, \bar{\mathbf{p}}, \mathbf{u}, t\right) = 0 \longrightarrow$ system dynamics

$\mathbf{x}(t_0) = \mathbf{x}_0 \longrightarrow$ initial conditions

$t \in [0, 240] \longrightarrow$ time

$\mathbf{p}_{\mathrm{L}} \leq \bar{\mathbf{p}} \leq \mathbf{p}_{\mathrm{U}} \longrightarrow$ parameter space

$\mathbf{u} = u_0 \longrightarrow$ input

- **non linear**
- **mixed-integer**
- **differential-algebraic constraints**
- **NP-complete**

Papoutsoglou G., Stamatiadou M., and Balas C., *IEEE iCBEB*, 2012

# In silico experimental setup

- **Test problem: 30 pseudo-experimental (PEX) curves.**
  - 10 manually selected,
    - represent all the clinical stages of neoplasia
  - 10 by step-wise sampling
  - 10 randomly selected
- **Two PEX data ensembles**
  - full set
  - reduced set
- **Exact results devoid of measurement noise**

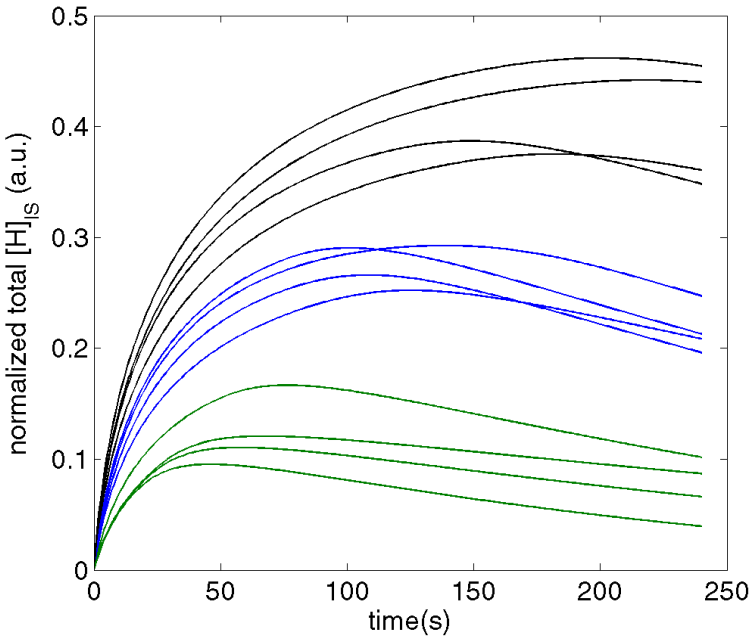


*Let the model be accurate and complete, then the validation of the solvability of the inverse problem is possible if repeatable convergence to unique solutions is achieved.*

# Performance estimation formulas

Each PEX curve is fitted 30 times ~9 hours (max)

## Parameter estimation accuracy

$$NRMSD(p)_k^{PE} = \frac{RMSD(p)_k^{PE}}{(p_{max} - p_{min})} = \frac{\sqrt{\sum_{i=1}^{30} \left(p_{i,k}^{PE} - \hat{p}_k^{PE}\right)^2}}{30 \cdot (p_{max} - p_{min})}$$

## Aggregate algorithmic accuracy per PEX

$$error_{al}^{PEX} = \sum_{i=1}^{k} \left\{ wg_i \times NRMSD(p_i)_{al}^{PEX} \right\}, \quad wg_i \cong \sum_{i=1}^{240} \frac{FOS(p_i)}{240}$$

8 parameters

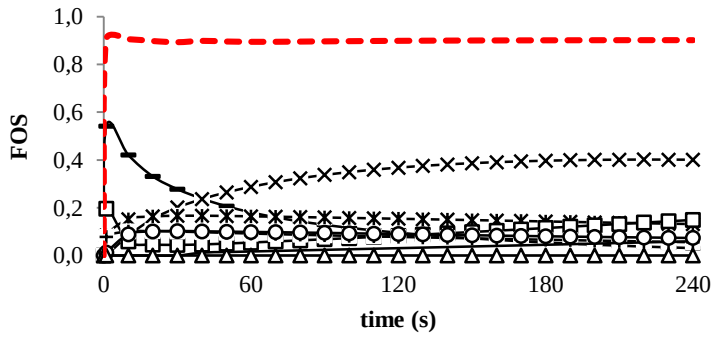


4 parameters

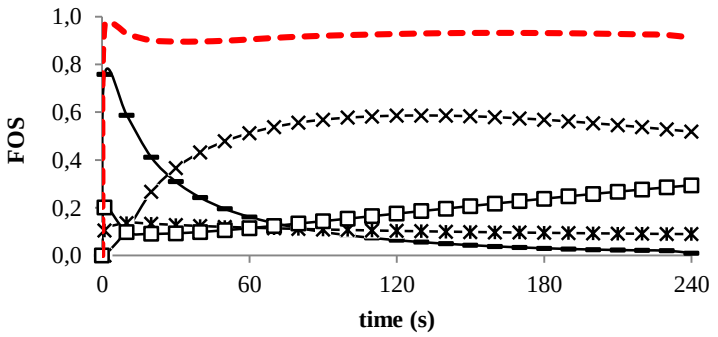

# Convergence efficiency

8 parameters

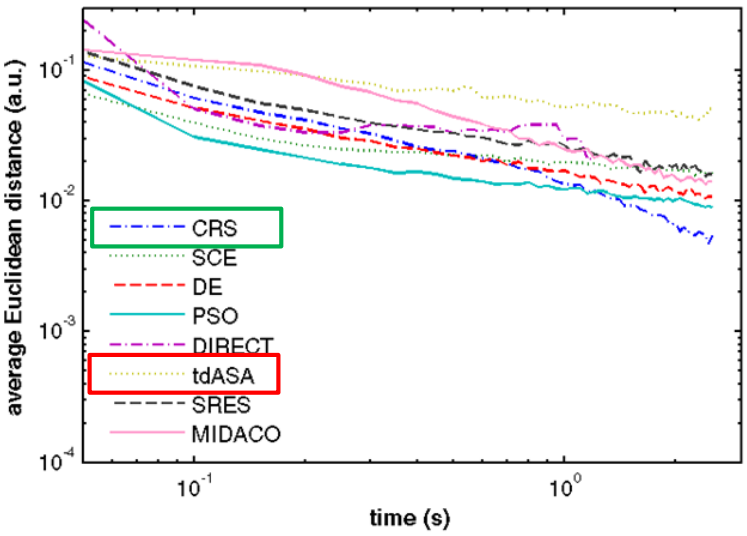


4 parameters

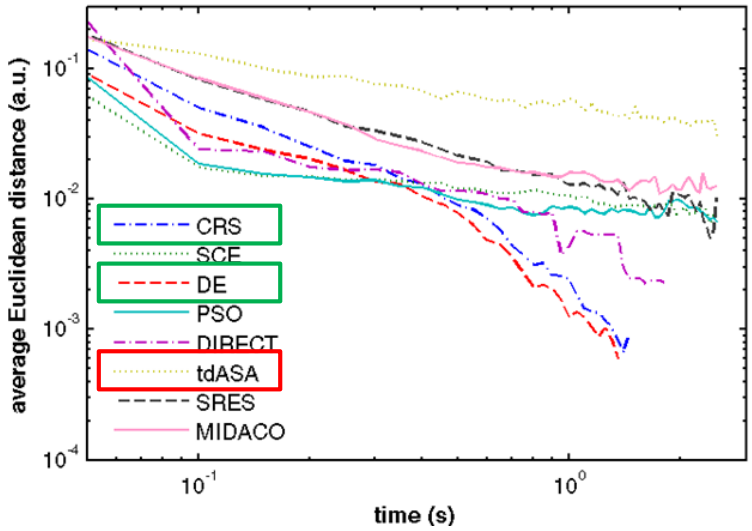


- Average Euclidean distance over all repetitive runs and all PEX data (every 3 seconds)

- **Full parameter case:** algorithms terminate most probably due to entrapment to locally optimum solutions
- **Reduced parameter case:** algorithms terminate most probably due to curve convergence

**Efficient :** CRSwCH, SCE, DE **//** **Inefficient:** tdASA, MIDACO, SRES

# Parameter estimation results

8 parameters

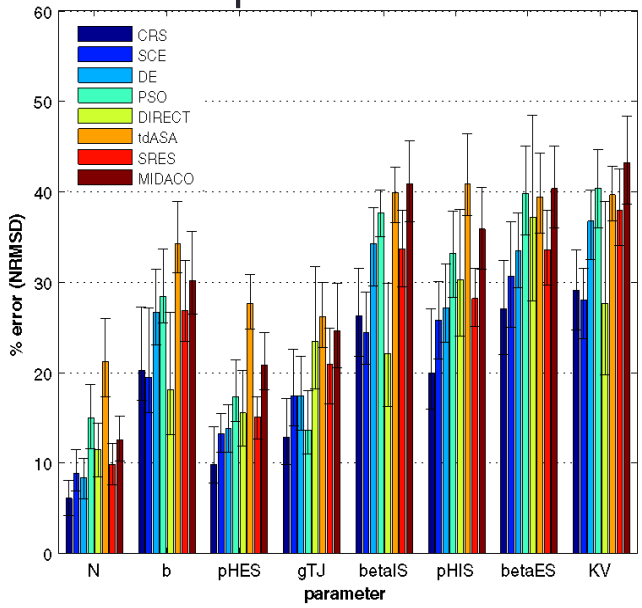


4 parameters

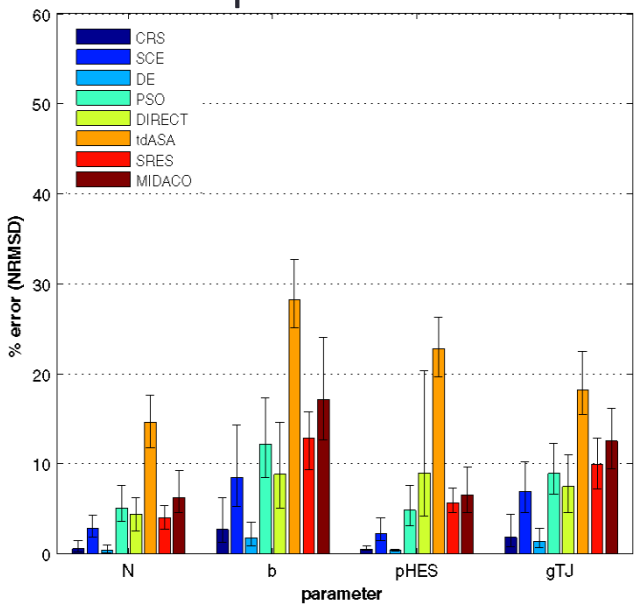


Aggregate estimation error (mean)

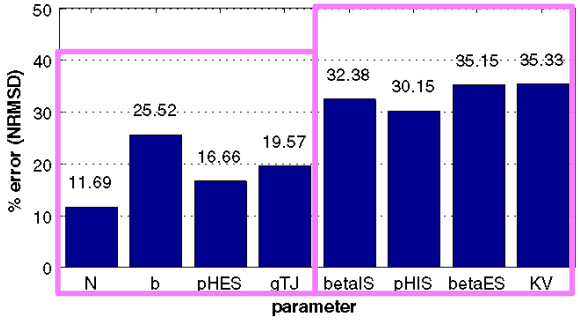


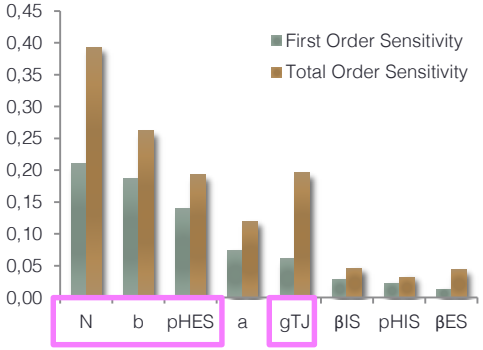


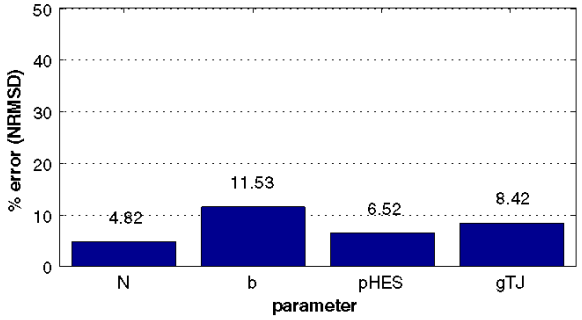


GSA validation

# Accuracy of the parameter estimations

- **high variance + outliers**
  - some algorithms have trouble to repeatedly reach a satisfactory low parameter estimation error
  - some PEX signals lead to more difficult optimization tasks
  - robustness: mean vs. median
- **Full parameter case**
  - many locally optimal solutions
  - fixing unimportant parameters is needed (GSA)
- **Reduced parameter case**
  - Low accuracy due to insufficient optimization time

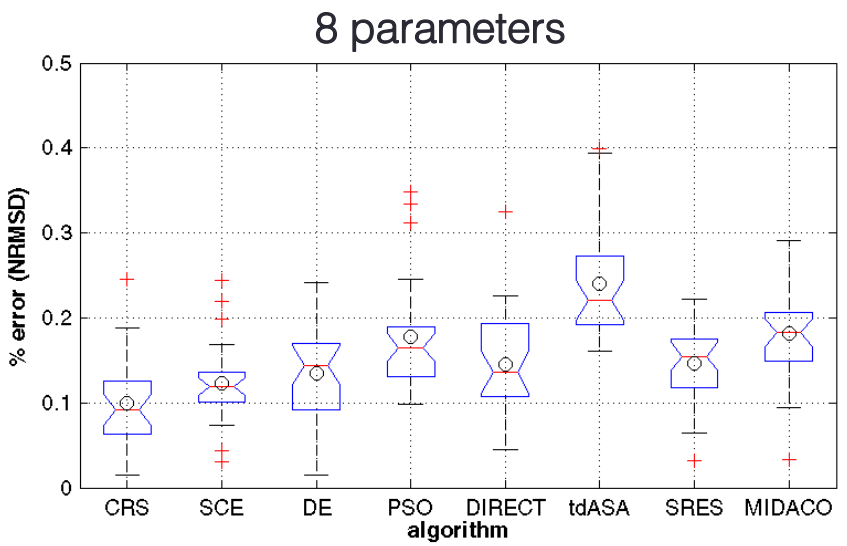


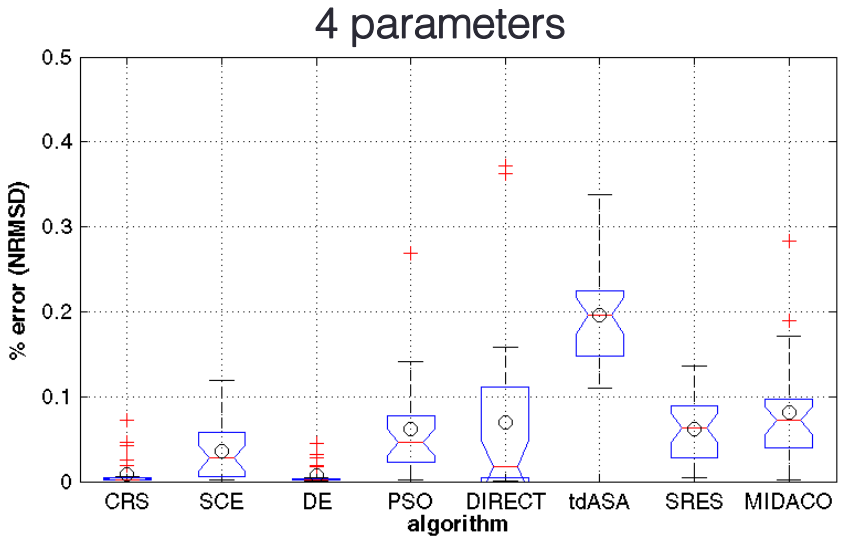

# Algorithm performance

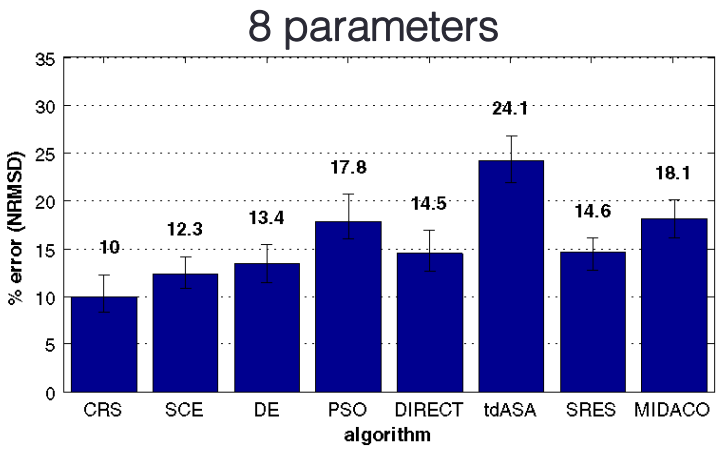


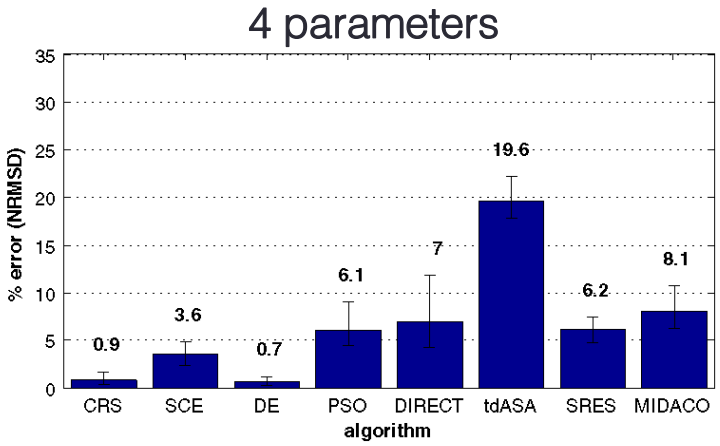


$$error_{al}^{PEX} = \sum_{i=1}^{k} \left\{ wg_i \times NRMSD(p_i)_{al}^{PEX} \right\},$$

## Student's *t*-test

| Algorithm | $\mu_{al} \leq 5\%$ *P*-value | $\mu_{al} \leq 5\%$ Hypothesis | $\mu_{al} \leq 8.5\%$ P-value | $\mu_{al} \leq 8.5\%$ Hypothesis |
|---|---|---|---|---|
| CRSwCH | $2{,}8 \cdot 10^{-42}$ | accepted | $4{,}7 \cdot 10^{-48}$ | accepted |
| SCE | 0,02 | accepted | $1{,}3 \cdot 10^{-08}$ | accepted |
| DE | $5{,}7 \cdot 10^{-43}$ | accepted | $1{,}0 \cdot 10^{-48}$ | accepted |
| PSO | 0,69 | *rejected* | 0,0002 | accepted |
| DIRECT | 0,46 | *rejected* | 0,0007 | accepted |
| tdASA | 1 | *rejected* | 1 | *rejected* |
| SRES | 0,95 | *rejected* | 0,0011 | accepted |
| MIDACO | 0,98 | *rejected* | 0,046 | accepted |

## Holm-Sidak multiple comparison test

| *i* | Test | *P*-value | *al i* | Hypothesis |
|---|---|---|---|---|
| 7 | DE – tdASA | 0.0000 | 0.0073 | *rejected* |
| 6 | DE – MIDACO | 0.0000 | 0.0085 | *rejected* |
| 5 | DE – DIRECT | 0.0000 | 0.0102 | *rejected* |
| 4 | DE – SRES | 0.0001 | 0.0127 | *rejected* |
| 3 | DE – PSO | 0.0001 | 0.0170 | *rejected* |
| 2 | DE – SCE | 0.0364 | 0.0253 | fail to reject |
| 1 | DE – CRSwCH | 0.8641 | - | accepted |

# Result 4: Solution of the inverse problem

- **The inverse problem is solvable using DE or CRSwCH methods**
- **Predicted value deviations ~1%**
  - high degree of convergence
  - almost unique set of parameters' for a given experimental curve
  - Statistical tests: it is unlikely for the predictions to have occurred by chance
- **The method is capable of estimating, with adequate accuracy, both structural and functional characteristics associated with the growth of epithelial neoplasia.**
- **Global optimization, computational biology and DCE-OI approaches have been employed together for the first time**

Conceptualization

Mathematical Implementation

Sensitivity Analysis

Solve the inverse

Parameter mapping

# THESIS RESULTS & CONTRIBUTIONS

# 5. IN VIVO MAPPING OF NEOPLASIA RELATED TISSUE PARAMETERS

Clinical data

Correlation of predictions with progresses of neoplasia

Parameter mapping

Interpretations

# Result 5: Mapping predictions

- **Concurrent estimation of the key biological parameters from *in vivo* measurements and for every spatial point is possible**
- **Our model is largely predictive**
  - no contradiction between our results and literature
- **Provide new insights in study of epithelial neoplasia**
- **We present a novel non invasive diagnostic method that contributes to cancer prevention.**

**Relevant publications**

G. Papoutsoglou, Theodoros-Marios Giakoumakis, and C. Balas, "*Dynamic contrast enhanced optical imaging of cervix, in vivo: A paradigm for mapping neoplasia-related parameters.*," in Conference proceedings : Annual International Conference of the IEEE Engineering in Medicine and Biology Society. Conference, Osaka, Japan, 2013, vol. 2013, pp. 3479–82

# Correlation of predictions with neoplasia growth (1)

- **Collect representative DR curves from each biopsy point (40)**
- **Fit using the best GO method**
  - Normalize
  - Data smoothing

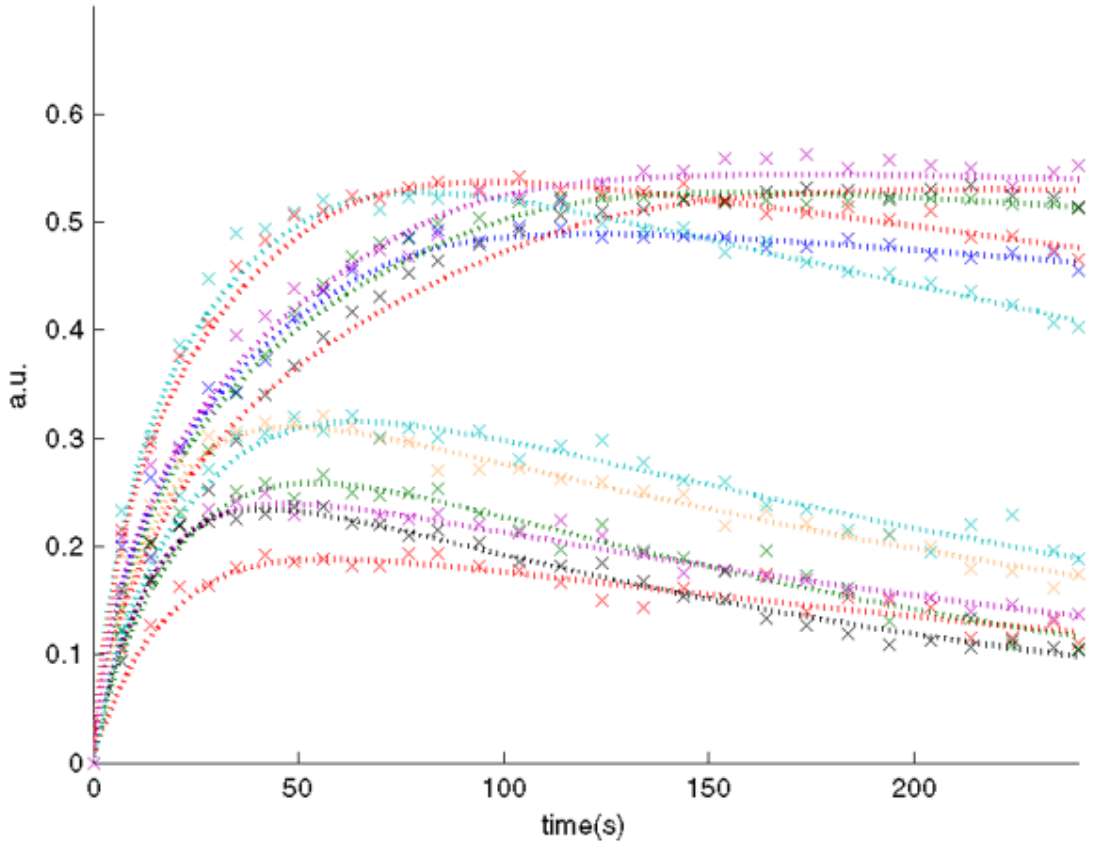

# Correlation of predictions with neoplasia growth (2)

- **N: high correlation**
  - neoplasia progression can be, in principle, predicted from the estimated values of the structural parameters such as the dysplastic cell packing
- ***b*: high correlation**
  - consistent with literature
  - results robustness
- **$pH_{ES}$: high correlation**
  - acid-mediated tumor invasion model
- **$g_{TJ}$: no significant correlation**
  - consistent with incoherent literature reports

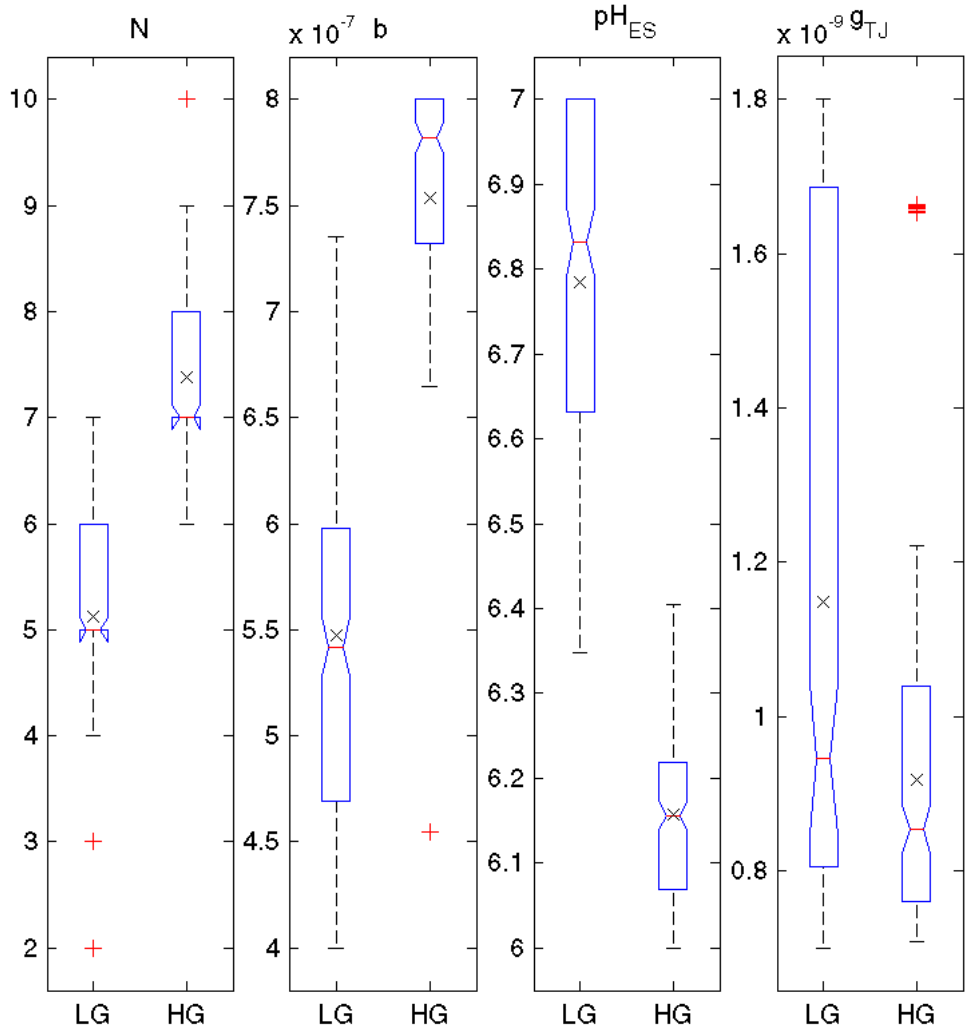

# High grade

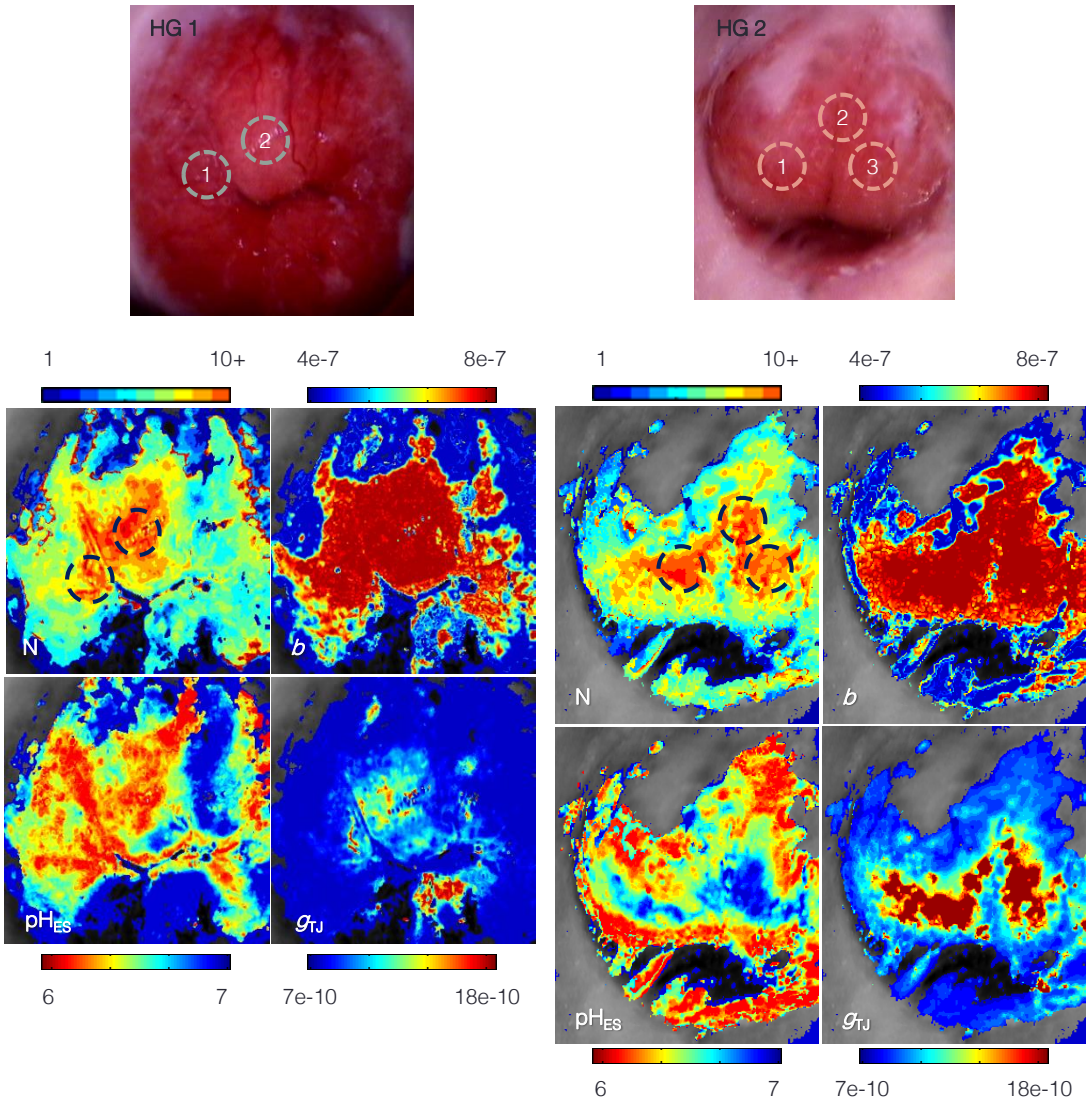


**N**

- high accumulation in HG areas
- size of lesion
  - additional criterion in colposcopy
- lesion within lesion
  - discriminate within the group of HG

***b***

- delineates the TZ
- atypical vasculature
  - mosaic pattern
  - punctuation
- diffusion areas

**$pH_{ES}$**

- cancer spreading
- invasion areas

**$g_{TJ}$**

- permittivity of tissue
- discriminate CIN II from III

# Low grade

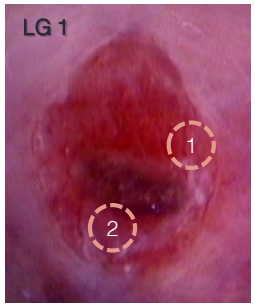


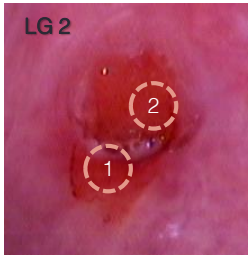


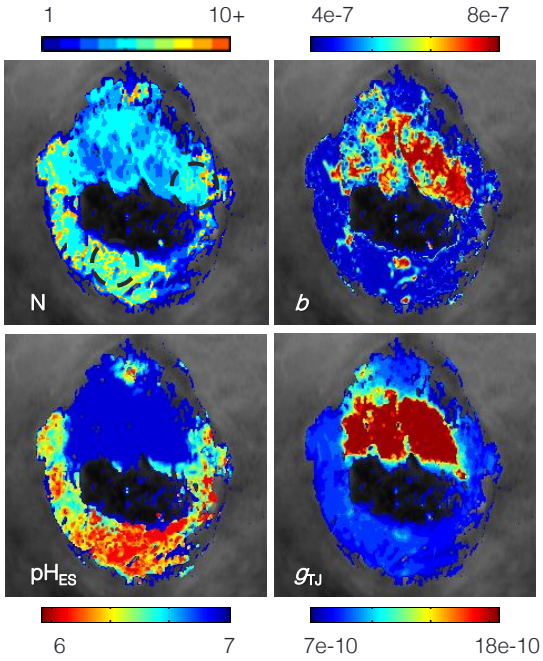


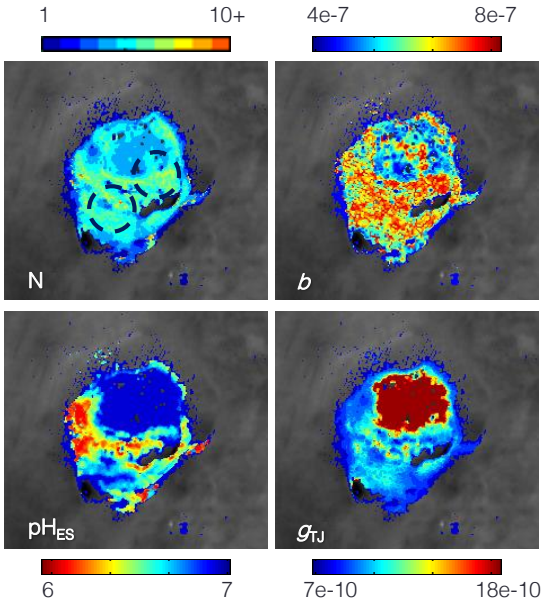


**N**

- low cell packing
- indistinct lesion
  - no sharp edges
  - no large tissue patches

***b***

- large ES exactly where biopsy is taken
  - method's sensitivity
- not excessive atypical vasculature
  - several color codes (metaplasia or LG)
- high values
  - pathogens
  - natural secretion or absorption

**$pH_{ES}$**

- exaggerate low values
  - columnar epithelium
  - slow onset of AW
- cancer spreading

**$g_{TJ}$**

- explains low $pH_{ES}$

# Result 5: Mapping predictions

- **Our predictions conforms to the biology of the cervix during the progression of neoplasia from LG to HG**
  - our model is largely, predictive
- **Concurrently estimated the key biological parameters from *in vivo* measurements and for every spatial point**
  - Our predictions for the number of dysplastic layers, which is the golden standard for histology classification, have been in total agreement with the doctors' assessments
  - Pseudocolor mappings are compatible with literature findings for both HG and LG neoplastic epithelia
  - Extract diagnostic information
- **We presented a novel non invasive diagnostic method that contributes to cancer prevention**
  - New insights in study of epithelial neoplasia
  - Can be exploited as a new optical biopsy technique
  - Detect the biodistribution and pharmacokinetic properties of contrast agents
  - Simply improve imaging of targeted contrast agents

# CONCLUSIONS

Summary

Ongoing research

Forward looking and further developments

# What we answered

- **Bio-Optical study**
  - Elucidated the origins of the dynamic optical phenomenon
- **Mathematical framework**
  - Developed a coherent model
  - Preliminary validation with experimental data
- **Sensitivity analysis**
  - Systematic reduction of model's complexity
  - most critical parameters with profound correlation with disease progression
- **Inverse problem solution**
  - In principle solvable
  - DE and CRSwCH are the most suitable algorithms
- **Parameter mapping**
  - Interpreted and correlated predictions and experimental results with literature and clinical practice
  - Added diagnostic information previously unattainable

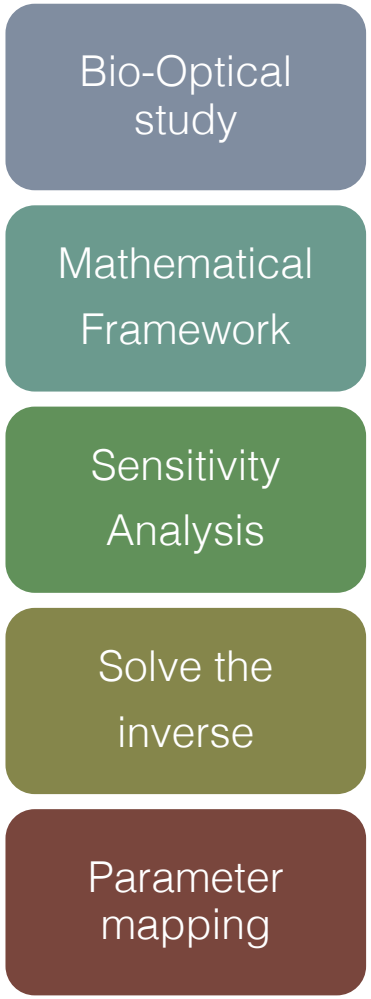


**Our novel methodology holds the promise to become the next paradigm shift in cancer screening**

# Ongoing research

- **Improvement of time complexity**
  - Lookup table
  - Create an approximate, analytic model
    - HDRM
  - Test combinations of local and global algorithms
    - DE + gblSolve
    - Kriging + gblSolve
  - Step-wise fitting using the estimability ratios

# Forward looking and further developments

- **Application to other markers and tissues (optical molecular imaging)**
  - Fluorescent dyes (ex vivo, in vitro)
  - Non toxic markers (in vivo)
  - Oral cavity, skin, larynx, Barrett's esophagus, lymphatic nodes, etc.
- **Integration with other imaging modalities**
  - fMRI
  - functional Ultrasound
  - Fluorescent imaging
  - etc.

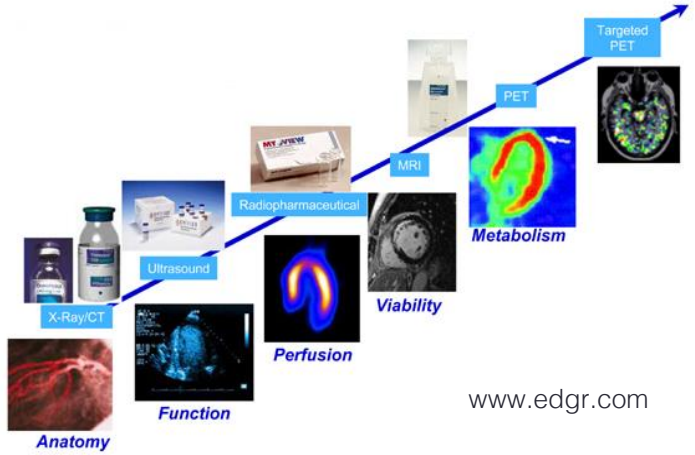


www.edgr.com

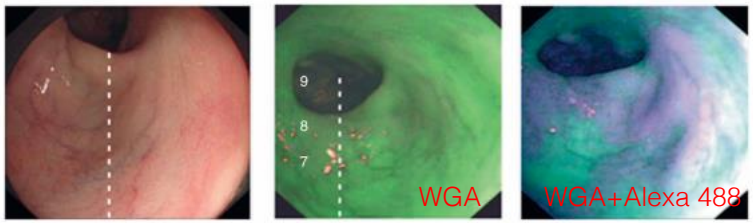


Bird-Lieberman, et al., *Nat. Med.*, 2012

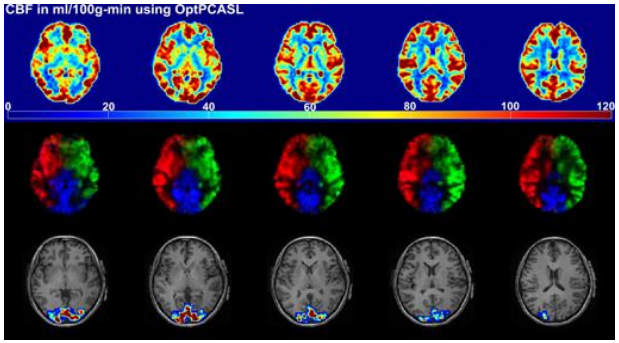


http://fmri.ucsd.edu/

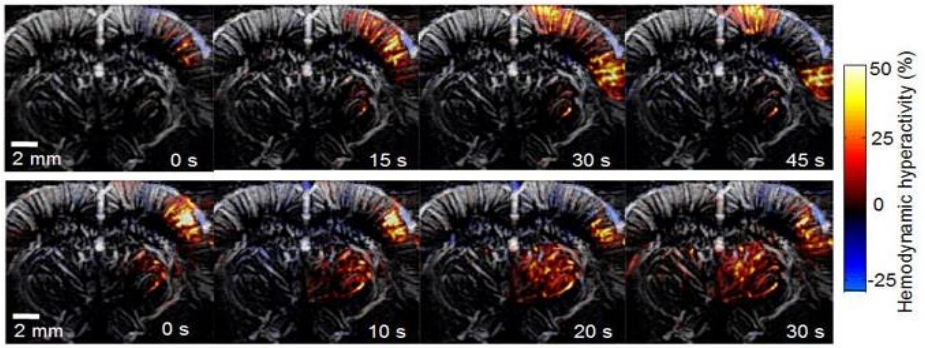


http://medicalphysicsweb.org

# Possible innovative derivative product

**Create a computational all-in-one suite that simulates pharmacodynamic/kinetic phenomena**

# Publications

## Journal

1. Papoutsoglou G. and Balas C., "*Estimation of Neoplasia-Related Biological Parameters through Modeling and Sensitivity Analysis of Optical Molecular Imaging Data*", IEEE Transactions on Biomedical Engineering, Vol. 60, No. 5, pp. 1241-1249, 2013
2. … (Journal of Biomedical Optics)

## Conference

1. Papoutsoglou G., Giakoumakis T.M. and Balas C., "*Dynamic Contrast Enhanced Optical Imaging of Cervix, in vivo: A Paradigm for Mapping Neoplasia-Related Parameters*," to be presented at the 35th Annual International Conference of the IEEE Engineering in Medicine and Biology Society (EMBC'13), 3-7 July, Osaka, Japan, 2013
2. Papoutsoglou G., Stamatiadou M., and Balas C., "*In silico modeling and global optimization of dynamic bio-optical processes for probing, in vivo, biological parameters of neoplasia*", International Conference on Biomedical Engineering and Biotechnology (iCBEB), 28-30 May, Macau, China, 2012
3. Papoutsoglou G., Anastasopoulou A., Stavrakakis G., Scouter P., Balas C., "*In Vivo Dynamic Imaging, in Silico Modeling and Global Sensitivity Analysis for the Study and the Diagnosis of Epithelial Neoplasia*," 33rd Annual International IEEE EMBS Conference, August 30 - September 3, Boston Marriott Copley Place, Boston, MA, USA, 2011
4. Balas C., Papoutsoglou G., Diakomanolis E. , Haidopoulos D. and Soutter W. P., "*Quantitative Assessment of the AW phenomenon and determination of its biophysical origins as a means for in vivo assessing CIN-related micro-structural and functional changes*," Journal of Lower Genital Tract Disease, vol. 14, pp. 264-269, ASCCP 2010 BIENNIAL MEETING, 24-27 March, Green Valley Ranch Resort, Las Vegas, NV, USA, 2010
5. Balas C., Papoutsoglou G., Loukas C., Skiadas Y., Pappas C., Haidopoulos D., Diakomanolis E., Soutter W.P., "*In vivo assessment of microstructural and functional alterations in cervical neoplasia", in the "Clinical and Biomedical Spectroscopy*" conference, part of the OSA/SPIE European Conferences on Biomedical Optics, 14-18 June, Munich, Germany, 2009
6. Balas C., Papoutsoglou G., Potirakis A. ,"*In Vivo Molecular Imaging of Cervical Neoplasia Using Acetic Acid as Biomarker*," IEEE Journal Of Selected Topics In Quantum Electronics, Vol. 14, No. 1, January/February, 2008

# Aknowledgements

**Antigoni Anastasopoulou**

the sensitivity

**Maria Stamatiadou**

the optimization

**Theodoros-Marios Giakoumakis**

the time complexity

NSRF - Research Funding Program: Heracleitus II. Investing in knowledge society through the European Social Fund.

Ευρωπαϊκή Ένωση
Ευρωπαϊκό Κοινωνικό Ταμείο

ΕΠΙΧΕΙΡΗΣΙΑΚΟ ΠΡΟΓΡΑΜΜΑ
ΕΚΠΑΙΔΕΥΣΗ ΚΑΙ ΔΙΑ ΒΙΟΥ ΜΑΘΗΣΗ
επένδυση στην κοινωνία της γνώσης
ΥΠΟΥΡΓΕΙΟ ΠΑΙΔΕΙΑΣ & ΘΡΗΣΚΕΥΜΑΤΩΝ, ΠΟΛΙΤΙΣΜΟΥ & ΑΘΛΗΤΙΣΜΟΥ
ΕΙΔΙΚΗ ΥΠΗΡΕΣΙΑ ΔΙΑΧΕΙΡΙΣΗΣ
Με τη συγχρηματοδότηση της Ελλάδας και της Ευρωπαϊκής Ένωσης

ΕΣΠΑ 2007-2013
πρόγραμμα για την ανάπτυξη
ΕΥΡΩΠΑΪΚΟ ΚΟΙΝΩΝΙΚΟ ΤΑΜΕΙΟ

# Thank you !!!

# APPENDIX

# Previous interpretations of the optical effect

- **occurs in**
  - the nucleus of the cell: coagulation/precipitation of nucleoproteins
    - Maclean A., Lower Genital Tract Neoplasia, 2003
  - cytoplasm: partial denaturation and possible polymerization of cytokeratins
    - S. Yamada, et al., Mol. Biol. Cell, 2002
- **occurs from**
  - weak acids
  - reversible and lasts < 4min
  - sodium acetate and dicarboxylic acids such as lactic acid are not producing the effect

# Maintaining the consistency of the results

- **Optimal tuning of intrinsic algorithm parameters**
  - Grid search
  - Literature
- **Algorithm surgery**
  - parallel coding (7-cores, MatlabTM's matlabpool() function)
  - integer value by truncation
- **Rules of fair comparison**
  - upper and lower bounds for the parameter values
  - common termination criteria
    - time or search effort: 2.5 minutes
    - curve convergence threshold (euclidean distance <10-3)
    - Population degenerates (geometric range < 10-3)
  - computation power
    - CPU: i7 2,66GHz, RAM: 8GB,
    - MatlabTM 2012a, Fortran 90
  - wherever applicable
    - sampling distributions
    - size of the initial population of search points

# Explanation of the calculated performances

- **stochastic methods**
  - no standard justification for the superior efficiency
  - no guarantees of optimality
  - cannot foresee the repeatability
  - possible explanation through the distinct features of each method
- **CRSwCH, DE, SCE**
  - simple, rely on the difference of parameter vectors
  - hybrid, several different mechanisms to evolve the potential solution candidates
  - adaptive switching between different mechanisms
- **PSO**
  - search is influenced by the points' neighborhoods
  - drive the population to local solutions
- **SRES**
  - complex mutation stage
  - slow down the search procedure
- **MIDACO**
  - Purely stochastic
- **tdASA**
  - traditionally not suitable for continuous variables
- **gblSolve**
  - expected low performance (deterministic algorithm)